Task Agnostic Continual Learning Using Online Variational Bayes with Fixed-Point Updates

Chen Zeno[1]**, Itay Golan**[1]**, Elad Hoffer** [2] **, Daniel Soudry** [1]

[1]Department of Electrical Engineering, Technion, Israel Institute of Technology, Haifa, Israel.

[2]Habana-Labs, Caesarea, Israel.

Keywords: continual learning, variational Bayes, catastrophic forgetting, neural networks.

Abstract

Background: Catastrophic forgetting is the notorious vulnerability of neural networks to the changes in the data distribution during learning. This phenomenon has long been considered a major obstacle for using learning agents in realistic continual learning settings. A large body of continual learning research assumes that task boundaries are known during training. However, only a few works consider scenarios in which task

boundaries are unknown or not well defined — task agnostic scenarios. The optimal Bayesian solution for this requires an intractable online Bayes update to the weights posterior.

Contributions: We aim to approximate the online Bayes update as accurately as possible. To do so, we derive novel fixed-point equations for the online variational Bayes optimization problem, for multivariate Gaussian parametric distributions. By iterating the posterior through these fixed-point equations, we obtain an algorithm (FOO-VB) for continual learning which can handle non-stationary data distribution using a fixed architecture and without using external memory (i.e. without access to previous data). We demonstrate that our method (FOO-VB) outperforms existing methods in task agnostic scenarios. FOO-VB Pytorch implementation is available at https://github.com/chenzeno/FOO-VB.

1   Introduction

Continual learning (CL) is the ability of an algorithm to learn from non-stationary data while reusing past knowledge and exploiting it to better adapt to a changing environment. A major challenge in continual learning is to overcome *catastrophic forgetting* (McCloskey and Cohen, 1989). Catastrophic forgetting is the tendency of neural networks to rapidly lose previously learned knowledge when the input distribution is changed abruptly, e.g. when changing a task or a source.

Neural networks are commonly used machine learning models for solving a variety of tasks. They are notorious for being vulnerable to changes in the data during learning. Various methods for preventing catastrophic forgetting in neural networks have been

suggested in the literature. Most of these methods assume relaxed conditions, in which the tasks arrive sequentially, and the data distribution changes only upon task-switches (i.e. piecewise stationary). Therefore, they are inapplicable in many realistic *task agnostic* applications, in which the tasks boundaries are unknown, or when such boundaries are not well-defined (e.g., the data distribution continuously changes in a non-stationary manner). For example, in image classification tasks in real-world scenarios, input images may exhibit several gradual changes through time, such as the zoom, illumination, or the angle of objects in the image. In this paper, we aim to reduce catastrophic forgetting in such difficult and relevant task agnostic cases.

It is long known that estimating the underlying posterior distribution can help mitigate catastrophic forgetting in neural networks (McCloskey and Cohen, 1989). Lately, it was found (Kirkpatrick et al., 2017) that one can use the posterior to find confidence levels for weights, which in turn can be used to affect the weight plasticity. That is to say, weights with a lower confidence value may be changed more in subsequent tasks (i.e., since they are "less important" for previous tasks). This allows a natural transition between learned tasks while reducing the ill effect of catastrophic forgetting. Later, Nguyen et al. (2017) also used variational Bayes to prevent catastrophic forgetting when the tasks arrive sequentially. In these works, each time a task switches, a new prior (or a regularization term) is added, which restricts the change of weights with high confidence (i.e., since they are "important" for previous tasks). However, in task agnostic scenarios this approach cannot be used, since the task boundary is unknown, or does not exist.

To prevent catastrophic forgetting in task agnostic scenarios, we propose using the online version of variational Bayes, which updates the approximate posterior using only

the current data sample without any knowledge on task switches. For the method to be effective, we aim to approximate the Bayes update as accurately as possible. Therefore, we derive novel fixed point equations for the online variational Bayes optimization problem under Gaussian parametric distributions (with either full, matrix variate, or diagonal covariance). Based on our theoretical results, for each Gaussian distribution, we propose the *Fixed-point Operator for Online Variational Bayes* (FOO-VB) algorithm. Our experiments demonstrate a significant improvement over existing algorithms in task agnostic continual learning scenarios.

2   Related Work

Bayesian neural networks   Bayesian inference for neural networks has been a subject of interest over many years. As exact Bayesian inference is intractable (for any realistic network size), much research has focused on approximation techniques. Most modern techniques stem from previous seminal works that used either a Laplace approximation (MacKay, 1992), variational methods (Hinton and Camp, 1993), or Monte Carlo methods (Neal, 1994). In recent years, many methods for approximating the posterior distribution have been suggested, falling into one of these categories. Those methods include assumed density filtering (Soudry et al., 2014; Hernández-Lobato and Adams, 2015), approximate power Expectation Propagation (Hernández-Lobato et al., 2016), Stochastic Langevin Gradient Descent (Welling and Teh, 2011; Balan et al., 2015), incremental moment matching (Lee et al., 2017), and variational Bayes (Graves, 2011; Blundell et al., 2015).

In this work, we focus on a variational Bayes approach. Practical variational Bayes for modern neural networks was first introduced by Graves (2011), where a parametric distribution was used to approximate the posterior distribution by minimizing the variational free energy. Calculating the variational free energy is intractable for general neural networks. Thus, Graves (2011) estimated the gradients using a biased Monte Carlo method, and used stochastic gradient descent (SGD) to perform minimization. In a later work, Blundell et al. (2015) used a re-parameterization trick to yield an unbiased estimator for the gradients. Variational Bayes methods were also used extensively on various probabilistic models including recurrent neural networks (Graves, 2011), auto-encoders (Kingma and Welling, 2013), and fully connected networks (Blundell et al., 2015). Martens and Grosse (2015); Zhang et al. (2017); Khan et al. (2018) suggested using the connection between natural gradient descent (Amari, 1998) and variational inference to perform natural gradient optimization in deep neural networks.

Fixed-point equations for the variation Bayes   In this work, we derive a novel fixed-point equation for the online variational Bayes optimization problem under Gaussian parametric distributions (with either full, matrix variate, or diagonal covariance) in the case of Bayesian neural networks. Fixed point equation for the variational Bayes optimization problem has been used in the cases of linear models (Knowles and Minka, 2011; Cseke et al., 2013) and Gaussian processes (Opper and Archambeau, 2009). Those derivations can not be used in the case of Bayesian neural networks. For instance, in the case of Gaussian processes, the negative log-likelihood of a single data point is a function of only one random variable (the parameter of the kernel function). So, the non-diagonal

elements of the posterior precision matrix are equal to those of the prior precision matrix, resulting in a closed-form solution to the posterior distribution. However, in the case of Bayesian neural networks, the negative log-likelihood of a single data point is a function of a random vector (the parameters vector). Another related work is Kurle et al. (2019), which suggested an algorithm for online inference for non-stationary streaming data. Kurle et al. (2019) derived the first-order necessary conditions for the online variational Bayes optimization problem in the case of Bayesian neural networks and multivariate Gaussian distribution. Kurle et al. (2019) used the first-order necessary conditions alongside a running memory to sequentially update the posterior parameters — but only in the case of a diagonal Gaussian distribution. However, as we will show here, using non-diagonal covariance can significantly improve performance.

Continual learning   Approaches for continual learning can be generally divided into four main categories: (1) Architectural approaches; (2) Rehearsal approaches; (3) Regularization approaches, and (4) Bayesian approaches.

Architectural approaches alter the network architecture to adapt to new tasks (e.g. Rusu et al. (2016); Nagabandi et al. (2018)). *Rehearsal approaches* use external memory[1] to allow re-training on stored examples from previous tasks (e.g. Shin et al. (2017)). *Regularization approaches* use some penalty on deviations from previous task weights. *Bayesian approaches* use Bayes' rule with the previous task posterior as the current prior. Each approach has pros and cons. For example, architectural approaches may result in extremely large architectures after multiple task switches. Rehearsal approaches may

---

[1]Rehearsal approaches may include GANs, which can be properly used as memory.

be problematic due to memory limitations or data availability (e.g. data from previous tasks may not be stored with the model due to privacy or proprietary reasons). For an extensive review of continual learning methods see Parisi et al. (2018). Our paper, however, focuses on *regularization* and *Bayesian approaches* where the architecture is fixed, and no external memory is used to retrain on data from previous tasks.

In *regularization* approaches, a regularization term is added to the loss function. *Elastic weight consolidation* (EWC) proposed by Kirkpatrick et al. (2017), slows changes in parameters that are important to the previous tasks by penalizing the difference between the previous task's optimal parameters and the current parameters. The importance of each parameter is measured using the diagonal of the Fisher information matrix. *Synaptic Intelligence* (SI) proposed by Zenke et al. (2017) also uses a penalty term, however, the importance is measured by the path length of updates on the previous task. Chaudhry et al. (2018) propose an online generalization of EWC and SI to achieve better performance. *Progress & compress* proposed by Schwarz et al. (2018) uses a network with two components (a knowledge base and an active column) with EWC for continual learning in reinforcement learning. *Memory Aware Synapses* (MAS) (Aljundi et al., 2018) also uses a penalty term, but measures weight importance by the sensitivity of the output function. *Learning without Forgetting* (LwF) proposed by Li and Hoiem (2017) uses knowledge distillation to enforce the network outputs of the new task to be similar to the network outputs of previous tasks.

The *Bayesian approaches* provide a solution to continual learning in the form of Bayes' rule. As data arrive sequentially, the posterior distribution of the parameters for the previous task is used as a prior for the new task. *Variational Continual Learning*

(VCL) proposed by Nguyen et al. (2017) uses online variational inference combined with the standard variational Bayes approach, *Bayes By Backprop* (BBB) by Blundell et al. (2015). They reduce catastrophic forgetting by replacing the prior on each task switch. In the BBB approach, a *mean-field approximation* is applied, assuming weights are independent of each other (i.e. the covariance matrix is diagonal). Ritter et al. (2018) suggests using Bayesian online learning with a Kronecker factored Laplace approximation to attain a non-diagonal method for reducing catastrophic forgetting. This allows the algorithm to exploit interactions between weights within the same layer.

Task-agnostic continual learning Most of the aforementioned methods, assume relaxed conditions, where tasks arrive sequentially, and the data distribution changes only on task switches. Few previous works deal with task agnostic scenarios (when task boundaries are unknown or not defined), however, they all use the rehearsal approach (Rao et al., 2019; Aljundi et al., 2019; Achille et al., 2018). We present an algorithm for task agnostic continual learning scenarios using a fixed architecture and without using external memory. Our work is orthogonal to those rehearsal approaches, and can potentially be combined with them.

3   General Theoretical Background

Bayesian inference (Gelman et al., 2013; Bishop et al., 1995) requires a joint probability distribution over the target set $\mathbf{D}$ and the model parameters $\boldsymbol{\theta}$ given the input set $\mathbf{X}$. This distribution can be written as

$$p\left(\mathbf{D}, \boldsymbol{\theta} | \mathbf{X}\right) = p\left(\mathbf{D} | \boldsymbol{\theta}, \mathbf{X}\right) p\left(\boldsymbol{\theta} | \mathbf{X}\right), \tag{1}$$

where $\mathbf{X} = \begin{bmatrix} \mathbf{x}_1 & \mathbf{x}_2 & \cdots & \mathbf{x}_N \end{bmatrix}^\top$ is the input set, $\mathbf{D} = \begin{bmatrix} \mathbf{y}_1 & \mathbf{y}_2 & \cdots & \mathbf{y}_N \end{bmatrix}^\top$ is the target set, and $\boldsymbol{\theta}$ is the model parameters vector. $p(\mathbf{D}|\boldsymbol{\theta}, \mathbf{X})$ is the likelihood function of the target set $\mathbf{D}$, and $p(\boldsymbol{\theta}|\mathbf{X})$ is the prior distribution of the model parameters $\boldsymbol{\theta}$. The posterior distribution of the model parameters can be calculated using Bayes' rule

$$p(\boldsymbol{\theta}|\mathbf{D}, \mathbf{X}) = \frac{p(\mathbf{D}|\boldsymbol{\theta}, \mathbf{X}) \, p(\boldsymbol{\theta}|\mathbf{X})}{p(\mathbf{D}|\mathbf{X})}, \tag{2}$$

where $p(\mathbf{D}|\mathbf{X})$ is calculated using the sum rule. To simplify the notations we omit the conditioning on $\mathbf{X}$ for the remainder of this paper.

We focus on the online version of Bayesian inference, in which the data arrive sequentially, and we update the posterior distribution whenever new data arrive. In each step, the previous posterior distribution is used as the new prior distribution. Therefore, according to Bayes' rule, the posterior distribution at time n is given by

$$p(\boldsymbol{\theta}|\mathbf{D}_n) = \frac{p(\mathbf{D}_n|\boldsymbol{\theta}) \, p(\boldsymbol{\theta}|\mathbf{D}_1, \cdots, \mathbf{D}_{n-1})}{p(\mathbf{D}_n)}, \tag{3}$$

Unfortunately, calculating the posterior distribution is intractable for most practical probability models, and especially when using deep neural networks. Therefore, we will use variational methods to approximate the true posterior.

Variational Bayes   In variational Bayes (Graves, 2011), a parametric distribution $q(\boldsymbol{\theta}|\phi)$ is used for approximating the true posterior distribution $p(\boldsymbol{\theta}|\mathbf{D})$ by (indirectly) minimizing the Kullback-Leibler (KL) divergence with the true posterior distribution

$$\mathcal{D}_{\mathrm{KL}}\left(q(\boldsymbol{\theta}|\phi)\,||\,p(\boldsymbol{\theta}|\mathbf{D})\right) = \mathbb{E}_{\boldsymbol{\theta} \sim q(\boldsymbol{\theta}|\phi)}\left[\log \frac{q(\boldsymbol{\theta}|\phi)}{p(\boldsymbol{\theta}|\mathbf{D})}\right]. \tag{4}$$

The optimal variational parameters (ϕ) are the solution of the following optimization problem:

$$\arg\min_{\phi} \int q\left(\boldsymbol{\theta}|\phi\right)\log\frac{q\left(\boldsymbol{\theta}|\phi\right)}{p\left(\boldsymbol{\theta}|\mathbf{D}\right)}d\boldsymbol{\theta} = \arg\min_{\phi} \int q\left(\boldsymbol{\theta}|\phi\right)\log\frac{q\left(\boldsymbol{\theta}|\phi\right)}{p\left(\mathbf{D}|\boldsymbol{\theta}\right)p\left(\boldsymbol{\theta}\right)}d\boldsymbol{\theta}$$

$$= \arg\min_{\phi} \mathbb{E}_{\boldsymbol{\theta}\sim q(\boldsymbol{\theta}|\phi)}\left[\log\left(q\left(\boldsymbol{\theta}|\phi\right)\right) - \log\left(p\left(\boldsymbol{\theta}\right)\right) + \mathrm{L}\left(\boldsymbol{\theta}\right)\right], \tag{5}$$

where $\mathrm{L}\left(\boldsymbol{\theta}\right) = -\log\left(p\left(\mathbf{D}|\boldsymbol{\theta}\right)\right)$ is the log-likelihood cost function.[2] The KL divergence between the parametric distribution (approximate posterior) and the true posterior distribution (4) is also known as the variational free energy.

In online variational Bayes (Broderick et al., 2013), one aims to find the posterior in an online setting, where data arrive sequentially. Similar to Bayesian inference, we use the previous approximated posterior as the new prior distribution, and the optimization problem becomes:

$$\arg\min_{\phi} \mathbb{E}_{\boldsymbol{\theta}\sim q_n(\boldsymbol{\theta}|\phi)}\left[\log\left(q_n(\boldsymbol{\theta}|\phi)\right) - \log\left(q_{n-1}(\boldsymbol{\theta})\right) + \mathrm{L}_n(\boldsymbol{\theta})\right]. \tag{6}$$

4   Proposed Theoretical Approach

We present a method to mitigate catastrophic forgetting in task agnostic continual learning. We aim to approximate the intractable (exact) online Bayes update rule (3) using the online variational Bayes optimization problem (6). Therefore, we use a new prior for each mini-batch (as in online variational Bayes) instead of using one prior for all the data (as in variational Bayes). When a Gaussian distribution is used as the parametric distribution $q\left(\boldsymbol{\theta}|\,\phi\right)$, one can find the fixed-point equations for the online variational

---

[2]Note that we define a cumulative log-likelihood cost function over the data.

Bayes optimization problem (6), i.e. the first-order necessary conditions. The fixed-point equations define the relation between the prior parameters and the posterior parameters. Using the fixed-point equations we derive algorithms for task agnostic continual learning (see section 5).

In the subsections to come, we derive novel fixed-point equations for the online variational Bayes (6) for multivariate Gaussian, Matrix variate Gaussian, and diagonal Gaussian distributions.

4.1   Fixed-point equations for multivariate Gaussian

In this subsection we focus on our most general case, in which the parametric distribution $q_n(\boldsymbol{\theta}|\phi)$ and the prior distribution $q_{n-1}(\boldsymbol{\theta})$ are multivariate Gaussian. Namely,

$$q_n(\boldsymbol{\theta}|\phi) = \mathcal{N}(\boldsymbol{\theta}|\boldsymbol{\mu}, \boldsymbol{\Sigma}), \quad q_{n-1}(\boldsymbol{\theta}) = \mathcal{N}(\boldsymbol{\theta}|\mathbf{m}, \mathbf{V}). \tag{7}$$

To find the fixed-point equations of the optimization problem in (6) in the case of a Gaussian distribution, we define the following deterministic transformation:

$$\boldsymbol{\theta} = \boldsymbol{\mu} + \mathbf{A}\boldsymbol{\epsilon}, \tag{8}$$

where $\phi = (\boldsymbol{\mu}, \boldsymbol{\Sigma}), \quad \boldsymbol{\Sigma} = \mathbf{A}\mathbf{A}^\top, \quad \boldsymbol{\epsilon} \sim \mathcal{N}(0, \mathbf{I}).$

Using the first-order necessary conditions on (6) for the optimal $\boldsymbol{\mu}$ and $\mathbf{A}$ (see Appendix 7 for details) we obtain the following equations

$$\boldsymbol{\mu} = \mathbf{m} - \mathbf{V}\mathbb{E}_{\boldsymbol{\epsilon}}[\nabla \mathrm{L}_n(\boldsymbol{\theta})], \quad \mathbf{A}\mathbf{A}^\top + \mathbf{V}\mathbb{E}_{\boldsymbol{\epsilon}}[\nabla \mathrm{L}_n(\boldsymbol{\theta})\boldsymbol{\epsilon}^\top]\mathbf{A}^\top - \mathbf{V} = 0. \tag{9}$$

In Lemma 1, we characterize the full set of solutions of the above quadratic equation (the proof can be found in Appendix 8).

Lemma 1. *Let* $\mathbf{T} \in \mathbb{R}^{N \times N}, \mathbf{M} \in \mathbb{R}^{N \times N}, \mathbf{M} = \mathbf{M}^\top, \mathbf{M} \succ 0, \mathbf{X} \in \mathbb{R}^{N \times N}$. *The full set of solutions of*

$$\mathbf{X}\mathbf{X}^\top + \mathbf{M}\mathbf{T}\mathbf{X}^\top - \mathbf{M} = 0 \tag{10}$$

is given by

$$\mathbf{X} = \mathbf{D}\mathbf{Q} - \frac{1}{2}\mathbf{M}\mathbf{T},$$

where

$$\mathbf{B} = \mathbf{M} + \frac{1}{4}\mathbf{M}\mathbf{T}\mathbf{T}^\top\mathbf{M}, \quad \mathbf{D} = \mathbf{B}^{1/2},$$

and $\mathbf{Q} \in \mathbb{R}^{N \times N}$ *is an orthogonal matrix such that* $\mathbf{D}\mathbf{Q}\mathbf{T}^\top\mathbf{M}$ *is a symmetric matrix.*

In Corollary 1 we demonstrate that Σ has a set of multiple solutions.

Corollary 1. *The full set of solutions for the optimal covariance matrix of the posterior distribution is given by*

$$\Sigma = \mathbf{V} + \frac{1}{2}\mathbf{V}\mathbb{E}_{\boldsymbol{\epsilon}}\left[\nabla\mathrm{L}_n\left(\boldsymbol{\theta}\right)\boldsymbol{\epsilon}^\top\right]\mathbb{E}_{\boldsymbol{\epsilon}}\left[\nabla\mathrm{L}_n\left(\boldsymbol{\theta}\right)\boldsymbol{\epsilon}^\top\right]^\top\mathbf{V}$$
$$- \frac{1}{2}\left(\mathbf{D}\mathbf{Q}\mathbb{E}_{\boldsymbol{\epsilon}}\left[\nabla\mathrm{L}_n\left(\boldsymbol{\theta}\right)\boldsymbol{\epsilon}^\top\right]^\top\mathbf{V} + \mathbf{V}\mathbb{E}_{\boldsymbol{\epsilon}}\left[\nabla\mathrm{L}_n\left(\boldsymbol{\theta}\right)\boldsymbol{\epsilon}^\top\right]\mathbf{Q}^\top\mathbf{D}^\top\right) \tag{11}$$

where

$$\mathbf{D} = \left(\mathbf{V} + \frac{1}{4}\mathbf{V}\mathbb{E}_{\boldsymbol{\epsilon}}\left[\nabla\mathrm{L}_n\left(\boldsymbol{\theta}\right)\boldsymbol{\epsilon}^\top\right]\mathbb{E}_{\boldsymbol{\epsilon}}\left[\nabla\mathrm{L}_n\left(\boldsymbol{\theta}\right)\boldsymbol{\epsilon}^\top\right]^\top\mathbf{V}\right)^{1/2} \tag{12}$$

and $\mathbf{Q}$ *is an orthogonal matrix such that* $\mathbf{D}\mathbf{Q}\mathbb{E}_{\boldsymbol{\epsilon}}\left[\nabla\mathrm{L}_n\left(\boldsymbol{\theta}\right)\boldsymbol{\epsilon}^\top\right]^\top\mathbf{V}$ *is a symmetric matrix.*

Next, we characterize a single solution for the quadratic equation using the following Lemma (the proof can be found in Appendix 9):

Lemma 2. *In this Lemma we use the notations of Lemma 1. Let* $\mathbf{Q} = \mathbf{S}\mathbf{W}^\top$ *such that* $\mathbf{S}, \mathbf{W}$ *are the left and right singular matrices of the Singular Value Decomposition (SVD) of* $\mathbf{D}^{-1}\mathbf{M}\mathbf{T}$. *Then* $\mathbf{Q}$ *is an orthogonal matrix and* $\mathbf{D}\mathbf{Q}\mathbf{T}^\top\mathbf{M}$ *is a symmetric matrix.*

Lemma 1 and 2 together reveal the fixed-point equations (we substitute $\mathbf{M} = \mathbf{V}$ and $\mathbf{T} = \mathbb{E}_{\boldsymbol{\epsilon}} \left[\nabla \mathrm{L}_n \left(\boldsymbol{\theta} \right) \boldsymbol{\epsilon}^\top \right]$)

$$\boldsymbol{\mu} = \mathbf{m} - \mathbf{V} \mathbb{E}_{\boldsymbol{\epsilon}} \left[\nabla \mathrm{L}_n \left(\boldsymbol{\theta} \right) \right], \quad \mathbf{A} = \mathbf{DQ} - \frac{1}{2} \mathbf{V} \mathbb{E}_{\boldsymbol{\epsilon}} \left[\nabla \mathrm{L}_n \left(\boldsymbol{\theta} \right) \boldsymbol{\epsilon}^\top \right] . \quad (13)$$

In case $\mathbf{B}$ is not invertible (or, more often, has a large condition number), the fixed-point equations can be derived using Lemma 3, which can be found in Appendix 10.

4.2 Fixed-point equations for matrix variate Gaussian

We now focus on the case in which the parametric distribution $q_n \left(\boldsymbol{\theta} | \phi \right)$ and the prior distribution $q_{n-1} \left(\boldsymbol{\theta} \right)$ are multivariate Gaussian whose covariance matrix is a Kronecker product of two PD matrices (Gupta and Nagar, 2018). This type of distribution is also known as Kronecker-factored Gaussian. Therefore:

$$q_n \left(\boldsymbol{\theta} | \phi \right) = \mathcal{N} \left(\boldsymbol{\theta} | \boldsymbol{\mu}, \boldsymbol{\Sigma}_1 \otimes \boldsymbol{\Sigma}_2 \right), \quad q_{n-1} \left(\boldsymbol{\theta} \right) = \mathcal{N} \left(\boldsymbol{\theta} | \mathbf{m}, \mathbf{V}_1 \otimes \mathbf{V}_2 \right), \quad (14)$$

where $\mathbf{V}_1, \boldsymbol{\Sigma}_1 \in \mathbb{R}^{d_1 \times d_1}$ (variance among-column) and $\mathbf{V}_2, \boldsymbol{\Sigma}_2 \in \mathbb{R}^{d_2 \times d_2}$ (variance among-row). To find the fixed-point equations of the optimization problem in (6) in the case of a matrix variate Gaussian distribution, we define a deterministic transformation

$$\boldsymbol{\theta} = \boldsymbol{\mu} + \left(\mathbf{A} \otimes \mathbf{B} \right) \boldsymbol{\epsilon} , \quad (15)$$

where the distribution parameters are $\phi = \left(\boldsymbol{\mu}, \boldsymbol{\Sigma}_1, \boldsymbol{\Sigma}_2 \right)$ and $\boldsymbol{\Sigma}_1 = \mathbf{A}\mathbf{A}^\top, \boldsymbol{\Sigma}_2 = \mathbf{B}\mathbf{B}^\top, \boldsymbol{\epsilon} \sim \mathcal{N} \left(0, \mathbf{I} \right)$.

We use the first-order necessary conditions for the optimal $\boldsymbol{\mu}, \mathbf{A}$, and $\mathbf{B}$ (see Ap-

pendix 11 for additional details)

$$\boldsymbol{\mu} = \mathbf{m} - (\mathbf{V}_1 \otimes \mathbf{V}_2) \, \mathbb{E}_{\boldsymbol{\epsilon}} \left[\nabla \mathrm{L}_n \left(\boldsymbol{\theta} \right) \right] \tag{16}$$

$$\mathrm{Tr} \left(\mathbf{V}_2^{-1} \boldsymbol{\Sigma}_2 \right) \mathbf{A} \mathbf{A}^\top + \mathbf{V}_1 \mathbb{E}_{\boldsymbol{\epsilon}} \left[\Psi^\top \mathbf{B} \Phi \right] \mathbf{A}^\top - p \mathbf{V}_1 = 0$$

$$\mathrm{Tr} \left(\mathbf{V}_1^{-1} \boldsymbol{\Sigma}_1 \right) \mathbf{B} \mathbf{B}^\top + \mathbf{V}_2 \mathbb{E}_{\boldsymbol{\epsilon}} \left[\Psi \mathbf{A} \Phi^\top \right] \mathbf{B}^\top - n \mathbf{V}_2 = 0 \,,$$

where $\Psi, \Phi \in \mathbb{R}^{p \times n}$ such that $\mathrm{vec}(\Psi) = \nabla \mathrm{L}_n \left(\boldsymbol{\theta} \right)$ and $\mathrm{vec}(\Phi) = \boldsymbol{\epsilon}$. In Appendix 13 we

use Lemma 2 to derive the fixed-point equations for (16).

4.3   Fixed-point equations for diagonal Gaussian

Now consider a parametric distribution $q \left(\boldsymbol{\theta} | \phi \right)$ and a prior distribution that are both

Gaussian with a diagonal covariance matrix (i.e. mean-field approximation). Therefore

$$q_n \left(\boldsymbol{\theta} | \phi \right) = \prod_i \mathcal{N} \left(\theta_i | \mu_i, \sigma_i^2 \right) , \quad q_{n-1} \left(\boldsymbol{\theta} \right) = \prod_i \mathcal{N} \left(\theta_i | m_i, v_i^2 \right) . \tag{17}$$

To derive the fixed-point equations of the optimization problem in (6), we once more

define a deterministic transformation

$$\theta_i = \mu_i + \epsilon_i \sigma_i \,, \tag{18}$$

where $\phi = \left(\boldsymbol{\mu}, \boldsymbol{\sigma} \right) , \quad \epsilon_i \sim \mathcal{N} \left(0, 1 \right).$

We use the first-order necessary conditions for the optimal μ_i and σ_i

$$\mu_i = m_i - v_i^2 \mathbb{E}_{\boldsymbol{\epsilon}} \left[\frac{\partial \mathrm{L}_n \left(\boldsymbol{\theta} \right)}{\partial \theta_i} \right] , \quad \sigma_i^2 + \sigma_i v_i^2 \mathbb{E}_{\boldsymbol{\epsilon}} \left[\frac{\partial \mathrm{L}_n \left(\boldsymbol{\theta} \right)}{\partial \theta_i} \epsilon_i \right] - v_i^2 = 0 \,. \tag{19}$$

Since this is a special case of (9) (where the covariance matrix is diagonal), one can use

(13) to derive the following fixed-point equations:

$$\mu_i = m_i - v_i^2 \mathbb{E}_\epsilon \left[\frac{\partial \mathrm{L}_n(\boldsymbol{\theta})}{\partial \theta_i} \right] \tag{20}$$

$$\sigma_i = v_i \sqrt{1 + \left(\frac{1}{2} v_i \mathbb{E}_\epsilon \left[\frac{\partial \mathrm{L}_n(\boldsymbol{\theta})}{\partial \theta_i} \epsilon_i \right] \right)^2} - \frac{1}{2} v_i^2 \mathbb{E}_\epsilon \left[\frac{\partial \mathrm{L}_n(\boldsymbol{\theta})}{\partial \theta_i} \epsilon_i \right].$$

5   Proposed Algorithms

5.1   From theory to practice

The fixed-point equations we derived in section 4 to the optimization problem (6) are only implicit solutions. Note for instance that the equations in (13) include the derivative $\nabla \mathrm{L}_n(\boldsymbol{\theta})$, which is a function of ϕ (the unknown posterior parameters). One possible approach to find a solution for the fixed-point equations is to iterate them. In certain simple linear models in offline variational Bayes, a similar approach can be proven to converge (Sheth and Khardon, 2016). Here, since we are at an online setting, we take a single explicit iteration of the fixed-point equation for each mini-batch, i.e. we evaluate the derivative $\nabla \mathrm{L}_n(\boldsymbol{\theta})$ using the prior parameters. This is done during the multiple passes through the data, as in Assumed Density Filter (ADF) (Soudry et al., 2014; Hernández-Lobato and Adams, 2015).

The fixed-point equations iteration consists of an expectation term w.r.t. ϵ. We use Monte Carlo samples to estimate those expectations.

5.2 Algorithms

FOO-VB   Using the relaxations above, we present the *Fixed-point operator for online variational Bayes* (FOO-VB) algorithmic framework (Algorithm 1), including three different specific variants: multivariate Gaussian, matrix variate Gaussian, and diagonal Gaussian (Algorithms 2, 3, and 4; the last two variants can be found in Appendix 15).

Algorithm 1 describes the general framework in which we update the posterior distribution as we iterate over the data. For each mini-batch we use K Monte Carlo samples of the neural network weights using the current prior distribution ϕ_{n-1} (steps 1 & 2), and then calculate the gradient w.r.t. these randomized weights (step 3). Lastly, we update the posterior parameters using the estimations and the update rules derived in section 4 (step 4).

Algorithm 1 Fixed-point operator for online variational Bayes (FOO-VB)

Initialize Prior parameters ϕ_0, Number of iterations N_{max},

   Number of Monte Carlo samples K

for $n = 1, \ldots, N_{max}$ sample a mini-batch

   for $k = 1, \ldots, K$

      Sample $\boldsymbol{\epsilon}^{(k)} \sim \mathcal{N}(0, \mathbf{I})$ {step 1}

      $\boldsymbol{\theta}^{(k)} = \text{TRANSFORM}\left(\boldsymbol{\epsilon}^{(k)}, \phi_{n-1}\right)$ {step 2}

      $\mathbf{g}^{(k)} = \nabla \mathrm{L}_n\left(\boldsymbol{\theta}^{(k)}\right)$ {step 3}

   end

   $\phi_n \leftarrow \text{UPDATE}\left(\phi_{n-1}, \boldsymbol{\epsilon}^{(1,\ldots,K)}, \mathbf{g}^{(1,\ldots,K)}\right)$ {step 4}

The deterministic transformation (step 2) and the posterior update rule (step 4) differ for each distribution. Algorithms 2, 3 and 4 described those steps for multivariate Gaussian, matrix variate Gaussian, and diagonal Gaussian, respectively (Algorithms 3 and 4 can be found in Appendix 15).

Algorithm 2 Methods for the multivariate Gaussian version

$\mathbf{TRANSFORM}(\boldsymbol{\epsilon}, \phi = (\boldsymbol{\mu}, \mathbf{A}))$:

$$\boldsymbol{\theta} = \boldsymbol{\mu} + \mathbf{A}\boldsymbol{\epsilon}$$

$$\boldsymbol{\Sigma} = \mathbf{A}\mathbf{A}^\top$$

$\mathbf{UPDATE}\left(\phi_{n-1} = (\boldsymbol{\mu}, \mathbf{A}), \boldsymbol{\epsilon}^{(1..K)}, \mathbf{g}^{(1..K)}\right)$:

$$\bar{\mathbf{E}}_1 = \tfrac{1}{K} \sum_{k=1}^{K} \mathbf{g}^{(k)}$$

$$\bar{\mathbf{E}}_2 = \tfrac{1}{K} \sum_{k=1}^{K} \mathbf{g}^{(k)} \left(\boldsymbol{\epsilon}^{(k)}\right)^\top$$

$$\boldsymbol{\mu} \leftarrow \boldsymbol{\mu} - \mathbf{A}\mathbf{A}^\top\bar{\mathbf{E}}_1$$

$$\mathbf{A} \leftarrow \mathbf{X} \text{ s.t. } \mathbf{X}\mathbf{X}^\top + \mathbf{A}\mathbf{A}^\top\bar{\mathbf{E}}_2\mathbf{X}^\top - \mathbf{A}\mathbf{A}^\top = 0$$

(This matrix equation is solved using Lemma 2)

Feasibility and complexity As Deep Neural Networks (DNN) often contain millions of parameters, it is infeasible to store the full covariance matrix between all parameters. A very common relaxation is to assume this distribution is factored between the layers (i.e. independent layers), so that the covariance matrix is a block diagonal matrix between layers. Even with this relaxation, the multivariate Gaussian version of FOO-VB is impractical due to memory limitations. For example, storing the matrix $\mathbf{A}$ for a fully

connected layer with 400 inputs and 400 outputs will require ~ 95GB (using 32-bit floating point).

We avoid working with such extremely large covariance matrices, by factoring them into a Kronecker product of two much smaller matrices (matrix variate Gaussian). Alternatively, we employ a diagonal covariance matrix (diagonal Gaussian).

The matrix variate Gaussian approximation enables us to store and apply mathematical operations on matrices of a practical size. For example, storing the matrices $\mathbf{A}$ and $\mathbf{B}$ of the matrix variate version for a fully connected layer with 400 inputs and 400 outputs will require ~ 1.2MB. In terms of runtime, this version requires four SVD decompositions for each layer in addition to the $K = 2500$ Monte-Carlo (MC) samples for each iteration. To reduce the runtime, one can parallelize the SVD (as in Berry and Sameh (1989)) and the MC sampling.

The diagonal approximation is our lightest version, with a memory footprint of only twice that of the regular network (to store the mean and variance of every weight). The $K = 10$ MC samples are the only overhead over a standard SGD optimizer, and so the runtime is linear w.r.t. the number of MC samples. See Appendix 17 for computational complexity analysis.

5.3   Theoretical properties of diagonal FOO-VB

We present theoretical properties of FOO-VB. For simplicity, we focus on the Diagonal Gaussian version. This version consists of a gradient descent algorithm for μ, and a recursive update rule for σ. The learning rate of μ_i is proportional to the uncertainty in the parameter θ_i according to the prior distribution. During the learning process, as more

data is seen, the learning rate decreases for parameters with a high degree of certainty, and increases for parameters with a high degree of uncertainty. Next, we establish this intuitive idea more precisely.

It is easy to verify that the update rule for σ is a strictly monotonically decreasing function of $\mathbb{E}_\epsilon \left[\frac{\partial \mathrm{L}_n(\boldsymbol{\theta})}{\partial \theta_i} \epsilon_i \right]$. Therefore

$$\mathrm{E}_\epsilon \left[\frac{\partial L(\boldsymbol{\theta})}{\partial \theta_i} \epsilon_i \right] > 0 \implies \sigma_i(n) < \sigma_i(n-1)$$

$$\mathrm{E}_\epsilon \left[\frac{\partial L(\boldsymbol{\theta})}{\partial \theta_i} \epsilon_i \right] < 0 \implies \sigma_i(n) > \sigma_i(n-1)$$

$$\mathrm{E}_\epsilon \left[\frac{\partial L(\boldsymbol{\theta})}{\partial \theta_i} \epsilon_i \right] = 0 \implies \sigma_i(n) = \sigma_i(n-1) . \tag{21}$$

Next, using a Taylor expansion for the loss, we show that for small values of σ, the quantity $\mathbb{E}_\epsilon \left[\frac{\partial \mathrm{L}_n(\boldsymbol{\theta})}{\partial \theta_i} \epsilon_i \right]$ is equal to

$$\mathbb{E}_\epsilon \left[\left(\frac{\partial \mathrm{L}_n(\mu)}{\partial \theta_i} + \sum_j \frac{\partial^2 \mathrm{L}_n(\mu)}{\partial \theta_i \partial \theta_j} \epsilon_j \sigma_j + O\left(\|\sigma\|^2\right) \right) \epsilon_i \right] = \frac{\partial^2 \mathrm{L}_n(\mu)}{\partial^2 \theta_i} \sigma_i + O\left(\|\sigma\|^2\right) ,$$

where we used $\mathbb{E}_\epsilon[\epsilon_i] = 0$ and $\mathbb{E}_\epsilon[\epsilon_i \epsilon_j] = \delta_{ij}$. Thus, in this case $\mathbb{E}_\epsilon \left[\frac{\partial \mathrm{L}_n(\boldsymbol{\theta})}{\partial \theta_i} \epsilon_i \right]$ is a finite difference approximation to the component-wise product of the diagonal of the Hessian of the loss and the vector σ. Therefore, we expect the uncertainty (learning rate) to decrease in areas with positive curvature (e.g., near local minima), or increase in areas with high negative curvature (e.g., near maxima, or saddles). This seems like a "sensible" behavior of the algorithm, since we wish to converge to local minima, but escape saddles. This in contrast to many common optimization methods, which are either insensitive to the sign of the curvature, or use it the wrong way (Dauphin et al., 2014).

In the case of a strongly convex loss, we prove a more rigorous statement in Appendix 14.

Theorem 1. *Consider FOO-VB with a diagonal Gaussian distribution for $\boldsymbol{\theta}$. If $\mathrm{L}_n(\boldsymbol{\theta})$ is a strongly convex function with parameter $m_n > 0$ and a continuously differentiable function over $\mathbb{R}^n$, then $\mathbb{E}_\epsilon \left[\frac{\partial \mathrm{L}_n(\boldsymbol{\theta})}{\partial \theta_i} \epsilon_i \right] \geq m_n \sigma_i > 0$.*

Corollary 2. *If $\mathrm{L}_n(\boldsymbol{\theta})$ is strongly convex (concave) for all $n \in \mathbb{N}$, then the sequence $\{\sigma_i(n)\}_{n=1}^\infty$ is strictly monotonically decreasing (increasing).*

Furthermore, one can generalize these results and show that if a restriction of $\mathrm{L}_n(\boldsymbol{\theta})$ to an axis θ_i is strongly convex (concave) for all $n \in \mathbb{N}$, then $\{\sigma_i(n)\}_{n=1}^\infty$ is monotonic decreasing (increasing).

Therefore, in the case of a strongly convex loss function, $\sigma_i = 0$ in any stable point of (20), which means that we collapse to point estimation similar to SGD. However, for neural networks, σ_i does not generally converge to zero. In this case, the stable point $\sigma_i = 0$ is generally not unique, since $\mathbb{E}_\epsilon \left[\frac{\partial \mathrm{L}(\boldsymbol{\theta})}{\partial \theta_i} \epsilon_i \right]$ implicitly depends on σ_i.

In Appendix 18 we show the histogram of STD (standard deviation) values on MNIST when training for 5000 epochs and demonstrate FOO-VB do not collapse to point estimation.

FOO-VB in continual learning   In the case of over-parameterized models and continual learning, only a part of the weights is essential for each task. We hypothesize that if a weight θ_i is important to the current task, this implies that near the minimum, the function $\mathrm{L}_i = \mathrm{L}(\boldsymbol{\theta})|_{(\boldsymbol{\theta})_i = \theta_i}$ is locally convex. Corollary 2 suggests that in this case σ_i would be small. In contrast, the loss will have a flat curvature in the direction of weights which are not important to the task. Therefore, these unimportant weights may have a large uncertainty σ_i. Since FOO-VB in the Diagonal Gaussian version introduces the

linkage between the learning rate and the uncertainty (STD), the training trajectories in the next task would be restricted along the less important weights leading to a good performance on the new task, while retaining the performance on the current task. The use of FOO-VB to continual learning exploits the inherent features of the algorithm, and it does not need any explicit information on tasks — it is completely unaware of the notion of tasks. We show empirical evidence for our hypothesis in subsection 6.1

6 Applications and Experiments

Inapplicability of other CL algorithms   In task-agnostic scenarios, previous optimization-based methods for continual learning are generally inapplicable, as they rely on taking some actions (e.g., changing parameters in the loss function) on task switch, which is undefined in those scenarios. Nevertheless, one possible adaptation is to take the core action at every iteration instead of at every task switch. Doing so is impractical for many algorithms due to the computational complexity, but for a fair comparison we have succeeded to run both Online EWC (Chaudhry et al., 2018) and MAS (Aljundi et al., 2018) with such an adaptation. As for rehearsal approach, it is orthogonal to our approach and can be combined. However, we focus on the challenging real-world scenario in which we do not have access to any data from previous tasks. Thus, in our experiments we do not compare to rehearsal algorithms.

We experiment on a task agnostic variations of the Permuted MNIST benchmark for continual learning. The Permuted MNIST benchmark is a set of tasks constructed by a random permutation of MNIST pixels. Each task has a different permutation of pixels

from the previous one. For all the experiments shown below, we conducted an extensive hyper-parameter search to find the best results for each algorithm. See additional details in Appendix 16.

6.1 Discrete task-agnostic Permuted MNIST

We evaluate the algorithms on a task-agnostic scenario where the task boundaries are unknown. To do so, we use the Permuted MNIST benchmark for continual learning, but without informing the algorithms on task switches. The network architecture is two hidden layers of width 100 (see additional details in Appendix 16). In Figure 1, we show the average test accuracy over all seen tasks as a function of the number of tasks. Designed for task agnostic scenarios, our algorithms surpass all other task agnostic algorithms. The matrix variate Gaussian version of FOO-VB experiences only $\sim 2\%$ degradation in the average accuracy after 10 tasks. The diagonal Gaussian version of FOO-VB attains a good balance between high accuracy ($\sim 88\%$ after 10 tasks) and low computational complexity.

The average test accuracy over all tasks at the end of training implies a good balance between remembering previous tasks while adapting to new tasks. On the other hand, in Figure 2 we show the test accuracy of the first task as a function of the number of seen tasks, which shows how well the algorithm remembers. The matrix variate Gaussian version of FOO-VB is being able to remember the first task almost perfectly (i.e. like the oracle), and the overall performance is limited only by the test accuracy of the current task. The diagonal Gaussian version of FOO-VB exhibits the next best performance, compared to other algorithms.
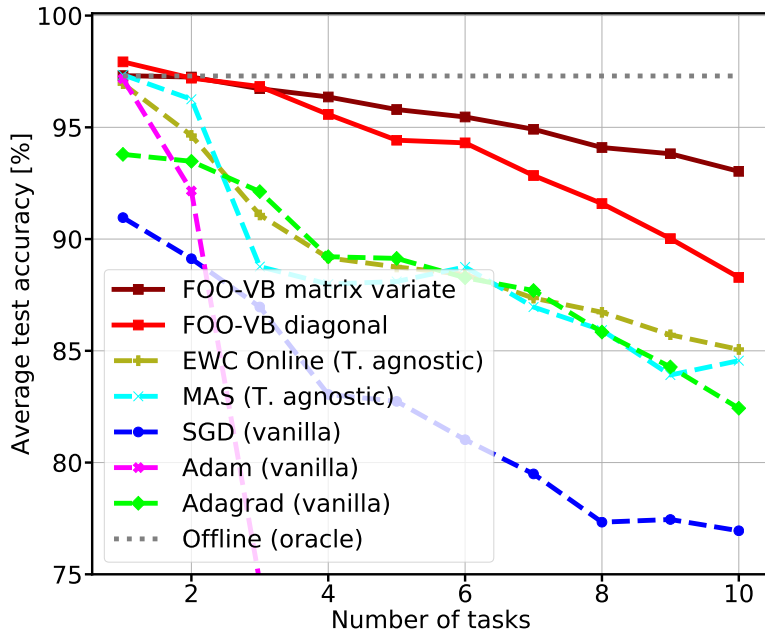
Figure 1: **Discrete task-agnostic Permuted MNIST:** The average test accuracy on all seen tasks as a function of the number of tasks. The hyper-parameters of all algorithms were tuned to maximize the average accuracy over all 10 tasks (therefore some of the algorithms have a relatively low accuracy for the first task). Offline (oracle) is a joint (i.e. not continual) training on all tasks.

We use the discrete task-agnostic Permuted MNIST experiment to examine our hypothesis of how the diagonal version of FOO-VB works in continual learning (subsection 5.3). Figure 3 shows the histogram of STD values at the end of the training process of each task. The results show that after the first task, a large portion of the weights have STD values close to the initial value 0.047, while a small fraction of them have a much lower value. As training progresses, more weights are assigned with STD values much lower than the initial value. These results support our hypothesis in subsection 5.3 that only a small part of the weights is essential for each task, and as training progresses more wights have low STD values.
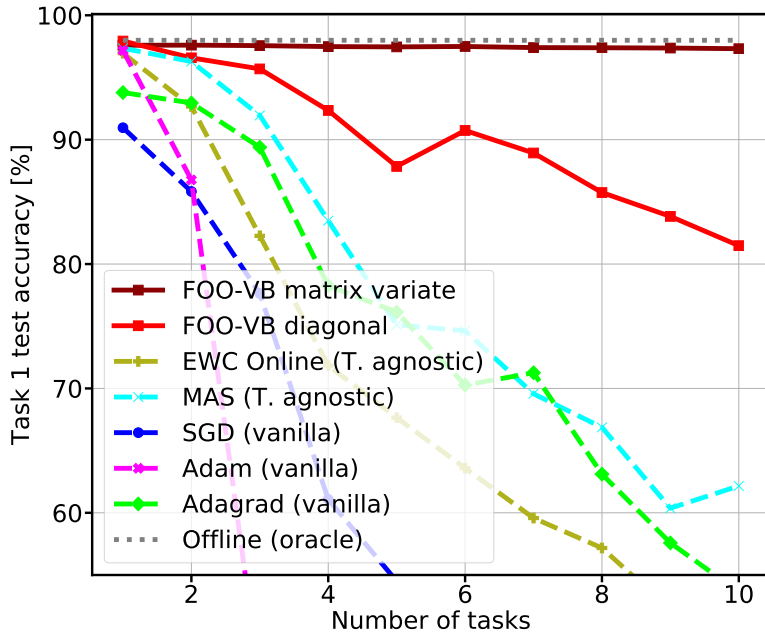
Figure 2: Test accuracy on the first task for discrete task-agnostic permuted MNIST. Oracle is the accuracy of training on task #1 only (i.e. not continual).

6.2 Continuous task-agnostic Permuted MNIST

We consider the case where the transition between tasks occurs gradually over time, so the algorithm gets a mixture of samples from two [3] different tasks during the transition (Figure 4) so the task boundaries are undefined. In all task-agnostic scenarios, the algorithm does not have any knowledge of the distribution over the tasks.

The network architecture is two hidden layers of width 200 (see additional details in Appendix 16). The output heads are shared among all tasks, task duration is $9380 \times T$ iterations, where $T = 10$ is the number of Tasks (corresponds to 20 epochs per task), and the algorithms are unaware to the number of tasks nor when the tasks are being switched.

---

[3]The most challenging scenario is when mixing two different tasks. As we add more tasks, we are getting closer to offline (non CL) training.
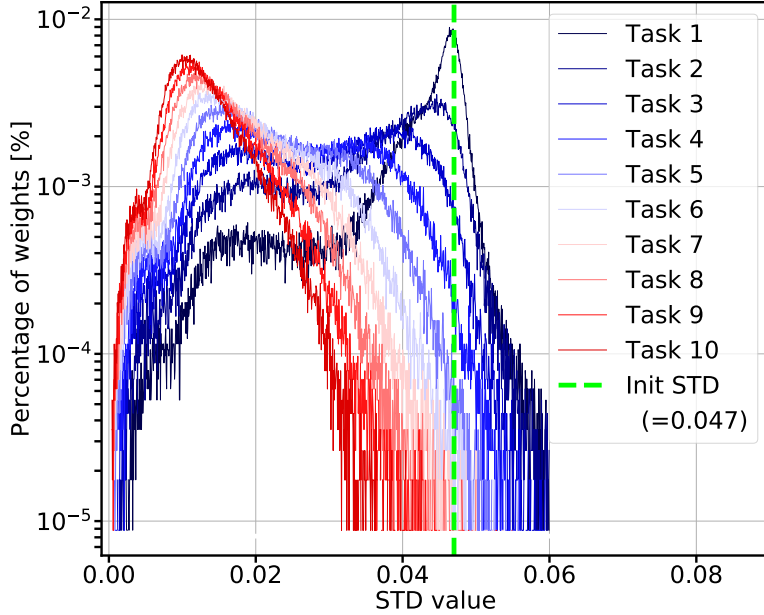
Figure 3: The histogram of STD values at the end of the training process of each task. As training progresses, more weights are assigned with STD values lower than the initial value. The initial STD value is 0.047. Best seen in color.

The average test accuracy over all tasks for different numbers of tasks is presented in Figure 5. As can be seen, the matrix variate Gaussian version of FOO-VB experiences less than 1% degradation in the average accuracy after 10 tasks. Similarly to the discrete task-agnostic experiment (subsection 6.1), the diagonal Gaussian version of FOO-VB maintains a good balance between high accuracy ($\sim 94\%$ after 10 tasks) and low computational complexity.

6.3   Task-aware continual learning on vision datasets

We provide additional evaluation of FOO-VB using the experiment of vision datasets conducted in Ritter et al. (2018). This experiment is done in the task-aware scenario, and uses more complex datasets (such as CIFAR10 and SVHN) and architecture (LeNet).
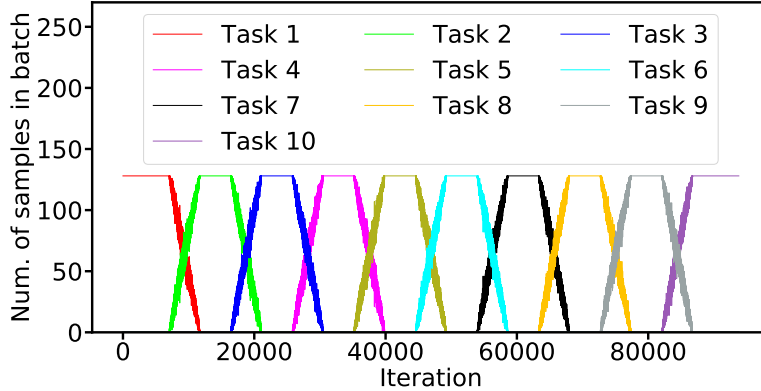
Figure 4: Distribution of samples from each task, as a function of iteration. The tasks are not changed abruptly but gradually – i.e. task boundaries are undefined. Here, the number of samples from each task in each batch is a random variable drawn from this distribution, which changes with time (iterations).

Thus, we use for this experiment the diagonal version of FOO-VB. The algorithms which FOO-VB is compared with are using the information on task-switch. Nevertheless, FOO-VB results are on par. See Appendix 19 for the full details.

Conclusion

In this work we aim to reduce catastrophic forgetting, in task agnostic scenarios (where task boundaries are unknown or not defined), using fixed architecture and without the use of external memory (i.e. without access to previous data, which can be restricted, e.g. due to privacy issues). This can allow deep neural networks to better adapt to new tasks without explicitly instructed to do so, enabling them to learn in real-world continual learning settings.
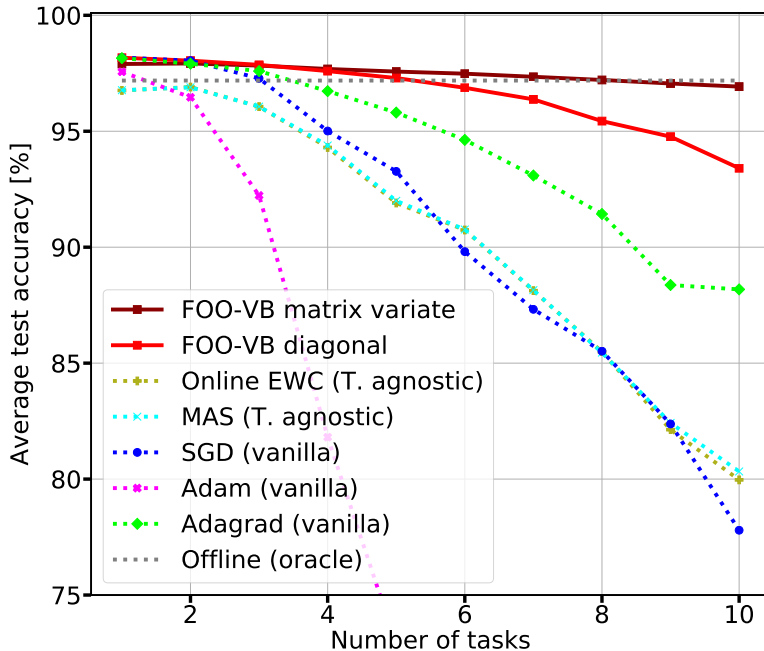
Figure 5: **Continuous task-agnostic Permuted MNIST:** The average test accuracy on all seen tasks as a function of the number of tasks. Tasks are changing gradually over time as showed in Figure 4. Offline (oracle) is a joint (not continual) training on all tasks.

Our method, FOO-VB, outperforms other continual learning methods in task agnostic scenarios. It relies on solid theoretical foundations, being derived from novel fixed-point equations of the online variational Bayes optimization problem. We derive two practical versions of the algorithm, to enable a trade-off between computational complexity vs. performance.

There are many possible extensions and use cases for FOO-VB which were not explored in this work. One possible extension is to incorporate FOO-VB in the framework of Meta-Learning (Finn et al., 2017) to address more challenging scenarios. Another direction is to use FOO-VB to improve GAN stability (Thanh-Tung and Tran, 2018). During the training process, the Discriminator exhibit catastrophic forgetting, since the

Generator output distribution changes gradually. FOO-VB fit this scenario naturally since it has no well defined task boundaries. Indeed, some of thus extensions were consider in He et al. (2019) using the diagonal version of FOO-VB (published in our preliminary pre-print (Zeno et al., 2019)). Last, but not least, FOO-VB could be potentially useful in reinforcement learning, which often includes non-stationary environments.

Acknowledgments

Appendix

7 Derivation of (9)

In this section, we provide additional details on the derivation of (9). The objective function is

$$
f\left(\boldsymbol{\mu}, \boldsymbol{\Sigma}\right) = \frac{1}{2}\left[\log\frac{\det\left(\mathbf{V}\right)}{\det\left(\boldsymbol{\Sigma}\right)} - N + \mathrm{Tr}\left(\mathbf{V}^{-1}\boldsymbol{\Sigma}\right) + \left(\mathbf{m} - \boldsymbol{\mu}\right)^{\top}\mathbf{V}^{-1}\left(\mathbf{m} - \boldsymbol{\mu}\right)\right] + \mathbb{E}_{\boldsymbol{\theta}}\left[\mathrm{L}_n\left(\boldsymbol{\theta}\right)\right].
$$

$$(22)$$

To solve the optimization problem in (6) in the case of Gaussian approximation, we use the deterministic transformation (8). To calculate the first derivative of the objective

function we use the following identities:

$$\mathbb{E}_{\boldsymbol{\theta}}\left[L_n\left(\boldsymbol{\theta}\right)\right] = \mathbb{E}_{\boldsymbol{\epsilon}}\left[L_n\left(\boldsymbol{\theta}\right)\right] \tag{23}$$

$$\frac{\partial \mathbb{E}_{\boldsymbol{\epsilon}}\left[L_n\left(\boldsymbol{\theta}\right)\right]}{\partial A_{i,j}} = \mathbb{E}_{\boldsymbol{\epsilon}}\left[\frac{\partial L_n\left(\boldsymbol{\theta}\right)}{\partial \theta_i}\epsilon_j\right] \tag{24}$$

$$\frac{\partial \operatorname{Tr}\left(\mathbf{V}^{-1}\boldsymbol{\Sigma}\right)}{\partial A_{i,j}} = 2\sum_n V_{i,n}^{-1} A_{n,j} \tag{25}$$

$$\frac{\partial \log|\det\left(\mathbf{A}\right)|}{\partial A_{i,j}} = A_{i,j}^{-\top}. \tag{26}$$

We use the first-order necessary conditions for the optimal $\boldsymbol{\mu}$:

$$-\mathbf{V}^{-1}\left(\mathbf{m}-\boldsymbol{\mu}\right) + \mathbb{E}_{\boldsymbol{\epsilon}}\left[\nabla L_n\left(\boldsymbol{\theta}\right)\right] = 0. \tag{27}$$

And so we obtained (9).

Next, we use the first-order necessary conditions for the optimal $\mathbf{A}$:

$$-\left(A^{-\top}\right)_{i,j} + \sum_n V_{i,n}^{-1} A_{n,j} + \mathbb{E}_{\boldsymbol{\epsilon}}\left[\frac{\partial L_n\left(\boldsymbol{\theta}\right)}{\partial \theta_i}\epsilon_j\right] = 0. \tag{28}$$

And in matrix form we obtain:

$$-\mathbf{A}^{-\top} + \mathbf{V}^{-1}\mathbf{A} + \mathbb{E}_{\boldsymbol{\epsilon}}\left[\nabla L_n\left(\boldsymbol{\theta}\right)\boldsymbol{\epsilon}^{\top}\right] = 0. \tag{29}$$

And so we obtained (9).

8 Proof of Lemma 1

The following proof is based on Poloni (2018).

Proof. Let

$$\mathbf{X} = \mathbf{DQ} - \frac{1}{2}\mathbf{MT}, \tag{30}$$

such that

$$\mathbf{B} = \mathbf{M} + \frac{1}{4}\mathbf{MTT}^\top\mathbf{M} \tag{31}$$

$$\mathbf{D} = \mathbf{B}^{1/2}. \tag{32}$$

If we compare (10) with its transpose we obtain

$$\mathbf{MTX}^\top = \mathbf{XT}^\top\mathbf{M}, \tag{33}$$

so we can rewrite (10) as follows,

$$\mathbf{XX}^\top + \frac{1}{2}\mathbf{MTX}^\top + \frac{1}{2}\mathbf{XT}^\top\mathbf{M} - \mathbf{M} = 0. \tag{34}$$

Next, we can factor (34) as follows,

$$\left(\mathbf{X} + \frac{1}{2}\mathbf{MT}\right)\left(\mathbf{X} + \frac{1}{2}\mathbf{T}^\top\mathbf{M}\right)^\top = \mathbf{M} + \frac{1}{4}\mathbf{MTT}^\top\mathbf{M}. \tag{35}$$

Since the matrix $\mathbf{B} = \mathbf{M} + \frac{1}{4}\mathbf{MTT}^\top\mathbf{M}$ is positive definite (PD)

$$\mathbf{D}^{-1}\left(\mathbf{X} + \frac{1}{2}\mathbf{MT}\right)\left(\mathbf{X} + \frac{1}{2}\mathbf{T}^\top\mathbf{M}\right)\mathbf{D}^{-1} = \mathbf{I}_N, \tag{36}$$

the equality holds if and only if $\mathbf{Q} = \mathbf{D}^{-1}\left(\mathbf{X} + \frac{1}{2}\mathbf{MT}\right)$ is an orthogonal matrix. In addition, the matrix

$$\mathbf{XT}^\top\mathbf{M} = \left(\mathbf{DQ} - \frac{1}{2}\mathbf{MT}\right)\mathbf{T}^\top\mathbf{M} = \mathbf{DQT}^\top\mathbf{M} - \frac{1}{2}\mathbf{MTT}^\top\mathbf{M} \tag{37}$$

is symmetric if and only if $\mathbf{DQT}^\top\mathbf{M}$ is symmetric. $\qquad\square$

9   Proof of Lemma 2

The following proof is based on Poloni (2018).

Proof. Let

$$\mathbf{Q} = \mathbf{SW}^\top \tag{38}$$

such that $\mathbf{S}, \mathbf{W}$ are the left and right singular matrices of the Singular Value Decomposition (SVD) of $\mathbf{D}^{-1}\mathbf{MT}$. Then

$$\mathbf{Q}^\top\mathbf{Q} = \mathbf{WS}^\top\mathbf{SW}^\top = \mathbf{I} \tag{39}$$

and

$$\mathbf{DQT}^\top\mathbf{M} = \mathbf{DSW}^\top\mathbf{T}^\top\mathbf{M} = \mathbf{DSW}^\top\mathbf{T}^\top\mathbf{MD}^{-\top}\mathbf{D}^\top \tag{40}$$

$$\overset{(a)}{=} \mathbf{DSW}^\top\mathbf{W\Lambda S}^\top\mathbf{D}^\top = \mathbf{DS\Lambda S}^\top\mathbf{D}^\top \tag{41}$$

where (a) is because $\mathbf{S}, \mathbf{W}$ are the left and right singular matrices of the SVD of $\mathbf{D}^{-1}\mathbf{MT}$ meaning, $\mathbf{D}^{-1}\mathbf{MT} = \mathbf{S\Lambda W}^\top$ and $\mathbf{\Lambda}$ is a diagonal matrix. Therefore $\mathbf{Q}$ is an orthogonal matrix and $\mathbf{DQT}^\top\mathbf{M}$ is a symmetric matrix. $\qquad\square$

10 Lemma 3

In this section, we derive a solution for (10) in the case where $\mathbf{B}$ is not invertible (or, more often, has a large condition number).

Lemma 3. *In this Lemma we use the notations of Lemma 1. Let* $\mathbf{Q} = \mathbf{UZ}^\top$ *such that* $\mathbf{U}, \mathbf{Z}$ *are the left singular matrices of the Generalized Singular Value Decomposition (GSVD) of* $\left(\mathbf{D}^\top, \mathbf{T}^\top\mathbf{M}\right)$*, respectively. Then* $\mathbf{Q}$ *is an orthogonal matrix and* $\mathbf{DQT}^\top\mathbf{M}$ *is a symmetric matrix.*

The following proof is based on Poloni (2018).

Proof. Let

$$\mathbf{Q} = \mathbf{S}\mathbf{W}^\top \tag{42}$$

such that $\mathbf{U}, \mathbf{Z}$ are the left singular matrices of the Generalized Singular Value Decomposition (GSVD) of $\left(\mathbf{D}^\top, \mathbf{T}^\top \mathbf{M}\right)$, respectively. Then

$$\mathbf{Q}^\top \mathbf{Q} = \mathbf{Z}\mathbf{U}^\top \mathbf{U}\mathbf{Z}^\top = \mathbf{I} \tag{43}$$

and

$$\mathbf{D}\mathbf{Q}\mathbf{T}^\top \mathbf{M} = \mathbf{D}\mathbf{U}\mathbf{Z}^\top \mathbf{T}^\top \mathbf{M} \overset{(a)}{=} \mathbf{W}\boldsymbol{\Lambda}_1 \mathbf{U}^\top \mathbf{U}\mathbf{Z}^\top \mathbf{Z}\boldsymbol{\Lambda}_2 \mathbf{W}^\top \tag{44}$$

$$= \mathbf{W}\boldsymbol{\Lambda}_1 \boldsymbol{\Lambda}_2 \mathbf{W}^\top \tag{45}$$

where (a) is because is because $\mathbf{U}, \mathbf{Z}$ are the left singular matrices of the GSVD of $\left(\mathbf{D}^\top, \mathbf{T}^\top \mathbf{M}\right)$ meaning, $\mathbf{D}^\top = \mathbf{U}\boldsymbol{\Lambda}_1 \mathbf{W}^\top, \mathbf{T}^\top \mathbf{M} = \mathbf{Z}\boldsymbol{\Lambda}_2 \mathbf{W}^\top$ and $\boldsymbol{\Lambda}_1, \boldsymbol{\Lambda}_2$ are diagonal matrices. Therefore $\mathbf{Q}$ is an orthogonal matrix and $\mathbf{D}\mathbf{Q}\mathbf{T}^\top \mathbf{M}$ is a symmetric matrix. $\quad\square$

11   Derivation of (16)

In this section, we provide additional details on the derivation of (16). The objective function is

$$f\left(\boldsymbol{\mu}, \boldsymbol{\Sigma}\right) = \frac{1}{2}\Bigg[\log \frac{\det\left(\mathbf{V}_1\right)^p \det\left(\mathbf{V}_2\right)^n}{\det\left(\boldsymbol{\Sigma}_1\right)^p \det\left(\boldsymbol{\Sigma}_2\right)^n} - np + \mathrm{Tr}\left(\left(\mathbf{V}_1 \otimes \mathbf{V}_2\right)^{-1}\left(\boldsymbol{\Sigma}_1 \otimes \boldsymbol{\Sigma}_2\right)\right) \tag{46}$$

$$+ \left(\mathbf{m} - \boldsymbol{\mu}\right)^\top \left(\mathbf{V}_1 \otimes \mathbf{V}_2\right)^{-1}\left(\mathbf{m} - \boldsymbol{\mu}\right)\Bigg]$$

$$+ \mathbb{E}_{\boldsymbol{\theta}}\left[\mathrm{L}_n\left(\boldsymbol{\theta}\right)\right]. \tag{47}$$

To solve the optimization problem in (6) in the case of Kronecker-factored approximation, we use the deterministic transformation (15). To calculate the first derivative of the

objective function we use the following identities (see Appendix 12 for additional details):

$$\frac{\partial \mathbb{E}_{\epsilon}\left[\mathrm{L}_n\left(\boldsymbol{\theta}\right)\right]}{\partial A_{i,j}} = \mathbb{E}_{\epsilon}\left[\sum_{\ell=1}^{p}\sum_{k=1}^{p}\frac{\partial \mathrm{L}_n\left(\boldsymbol{\theta}\right)}{\partial \theta_{\ell+(i-1)p}}B_{\ell,k}\boldsymbol{\epsilon}_{k+(j-1)p}\right] \tag{48}$$

$$\frac{\partial \mathbb{E}_{\epsilon}\left[\mathrm{L}_n\left(\boldsymbol{\theta}\right)\right]}{\partial B_{i,j}} = \mathbb{E}_{\epsilon}\left[\sum_{\ell=1}^{n}\sum_{k=1}^{n}\frac{\partial \mathrm{L}_n\left(\boldsymbol{\theta}\right)}{\partial \theta_{i+(\ell-1)n}}A_{\ell,k}\boldsymbol{\epsilon}_{j+(k-1)n}\right] \tag{49}$$

$$\mathrm{Tr}\left(\left(\mathbf{V}_1\otimes\mathbf{V}_2\right)^{-1}\left(\boldsymbol{\Sigma}_1\otimes\boldsymbol{\Sigma}_2\right)\right) = \mathrm{Tr}\left(\mathbf{V}_1^{-1}\boldsymbol{\Sigma}_1\right)\mathrm{Tr}\left(\mathbf{V}_2^{-1}\boldsymbol{\Sigma}_2\right). \tag{50}$$

We use the first-order necessary conditions for the optimal $\boldsymbol{\mu}$:

$$- \left(\mathbf{V}_1\otimes\mathbf{V}_2\right)^{-1}\left(\mathbf{m}-\boldsymbol{\mu}\right) + \mathbb{E}_{\epsilon}\left[\nabla\mathrm{L}_n\left(\boldsymbol{\theta}\right)\right] = 0. \tag{51}$$

And so we obtained (16). We use the first-order necessary conditions for the optimal $\mathbf{A}$:

$$-p\left(A^{-\top}\right)_{i,j} + \mathrm{Tr}\left(\mathbf{V}_2^{-1}\boldsymbol{\Sigma}_2\right)\sum_k(V_1)_{i,k}^{-1}A_{k,j} + \mathbb{E}_{\epsilon}\left[\sum_{\ell=1}^{p}\sum_{k=1}^{p}\frac{\partial \mathrm{L}_n\left(\boldsymbol{\theta}\right)}{\partial \theta_{\ell+(i-1)p}}B_{\ell,k}\boldsymbol{\epsilon}_{k+(j-1)p}\right] = 0. \tag{52}$$

And in matrix form we obtain:

$$-p\mathbf{A}^{-\top} + \mathrm{Tr}\left(\mathbf{V}_2^{-1}\boldsymbol{\Sigma}_2\right)\mathbf{V}_1^{-1}\mathbf{A} + \mathbb{E}_{\epsilon}\left[\Psi^{\top}\mathbf{B}\Phi\right] = 0. \tag{53}$$

where $\Psi, \Phi \in \mathbb{R}^{p\times n}$ such that $\mathrm{vec}(\Psi) = \nabla\mathrm{L}_n\left(\boldsymbol{\theta}\right)$ and $\mathrm{vec}(\Phi) = \boldsymbol{\epsilon}$. And so we obtained (16).

We use the first-order necessary conditions for the optimal $\mathbf{B}$:

$$-n\left(B^{-\top}\right)_{i,j} + \mathrm{Tr}\left(\mathbf{V}_1^{-1}\boldsymbol{\Sigma}_1\right)\sum_k(V_2)_{i,k}^{-1}B_{k,j} + \mathbb{E}_{\epsilon}\left[\sum_{\ell=1}^{n}\sum_{k=1}^{n}\frac{\partial \mathrm{L}_n\left(\boldsymbol{\theta}\right)}{\partial \theta_{i+(\ell-1)n}}A_{\ell,k}\boldsymbol{\epsilon}_{j+(k-1)n}\right] = 0. \tag{54}$$

And in matrix form we obtain:

$$-n\mathbf{B}^{-\top} + \mathrm{Tr}\left(\mathbf{V}_1^{-1}\boldsymbol{\Sigma}_1\right)\mathbf{V}_2^{-1}\mathbf{B} + \mathbb{E}_{\epsilon}\left[\Psi^{\top}\mathbf{A}\Phi\right] = 0. \tag{55}$$

And so we obtained (16).

12   Technical results for Appendix 11

In this section, we prove the technical results used in Appendix 11.

Let $\Delta_{i,j}^{(n)} \in \mathbb{R}^{n\times n}$ such that

$$(\Delta_{i,j}^{(n)})_{n,m} = \delta_{n,i}\delta_{m,j}.$$

We then have

$$
\begin{aligned}
\frac{\partial \mathbb{E}_{\epsilon}\left[\mathrm{L}_n\left(\boldsymbol{\theta}\right)\right]}{\partial A_{i,j}} &= \mathbb{E}_{\epsilon}\left[\frac{\partial \mathrm{L}_n\left(\boldsymbol{\theta}\right)}{\partial A_{i,j}}\right] \\
&\stackrel{\text{(a)}}{=} \mathbb{E}_{\epsilon}\left[\sum_{\ell=1}^{np}\frac{\partial \mathrm{L}_n\left(\boldsymbol{\theta}\right)}{\partial \theta_\ell}\cdot\frac{\partial \theta_\ell}{\partial A_{i,j}}\right] \\
&\stackrel{\text{(b)}}{=} \mathbb{E}_{\epsilon}\left[\sum_{\ell=1}^{np}\frac{\partial \mathrm{L}_n\left(\boldsymbol{\theta}\right)}{\partial \theta_\ell}\cdot\frac{\partial(\mu_\ell+\sum_k(\mathbf{A}\otimes\mathbf{B})_{\ell,k}\epsilon_k)}{\partial A_{i,j}}\right] \\
&\stackrel{\text{(c)}}{=} \mathbb{E}_{\epsilon}\left[\sum_{\ell=1}^{np}\frac{\partial \mathrm{L}_n\left(\boldsymbol{\theta}\right)}{\partial \theta_\ell}\sum_{k=1}^{np}\left(\Delta_{i,j}^{(n)}\otimes\mathbf{B}\right)_{\ell,k}\epsilon_k\right] \\
&\stackrel{\text{(d)}}{=} \mathbb{E}_{\epsilon}\left[\sum_{\ell=(i-1)p+1}^{ip}\frac{\partial \mathrm{L}_n\left(\boldsymbol{\theta}\right)}{\partial \theta_\ell}\sum_{k=(j-1)p+1}^{jp}\left(\Delta_{i,j}^{(n)}\otimes\mathbf{B}\right)_{\ell,k}\epsilon_k\right] \\
&= \mathbb{E}_{\epsilon}\left[\sum_{\ell=1}^{p}\sum_{k=1}^{p}\frac{\partial \mathrm{L}_n\left(\boldsymbol{\theta}\right)}{\partial \theta_{\ell+(i-1)p}}B_{\ell,k}\epsilon_{k+(j-1)p}\right],
\end{aligned}
\tag{56}
$$

where

- (a) is because $\boldsymbol{\theta}$ is a vector of length $n\cdot p$ and by the chain rule for derivatives;

- (b) holds since $\theta_\ell = \mu_\ell + \sum_{k=1}^{np}(\mathbf{A}\otimes\mathbf{B})_{\ell,k}\,\epsilon_k$;

- (c) is by definition of $\Delta_{i,j}^{(n)}$, and since we differentiate by $A_{i,j}$;

- (d) is since $(\Delta_{i,j}^{(n)}\otimes\mathbf{B})_{\ell,k} \neq 0$ if $(i-1)p+1 \le \ell \le ip$ or if $(j-1)p+1 \le k \le jp$.

Let $\Delta_{i,j}^{(p)} \in \mathbb{R}^{p\times p}$ such that

$$(\Delta_{i,j}^{(p)})_{n,m} = \delta_{n,i}\delta_{m,j}.$$

34

We then have

$$
\begin{aligned}
\frac{\partial \mathbb{E}_{\boldsymbol{\epsilon}}\left[\mathrm{L}_n\left(\boldsymbol{\theta}\right)\right]}{\partial B_{i,j}} &= \mathbb{E}_{\boldsymbol{\epsilon}}\left[\frac{\partial \mathrm{L}_n\left(\boldsymbol{\theta}\right)}{\partial B_{i,j}}\right] \\
&\overset{\text{(a)}}{=} \mathbb{E}_{\boldsymbol{\epsilon}}\left[\sum_{\ell=1}^{np} \frac{\partial \mathrm{L}_n\left(\boldsymbol{\theta}\right)}{\partial \theta_\ell} \cdot \frac{\partial \theta_\ell}{\partial B_{i,j}}\right] \\
&\overset{\text{(b)}}{=} \mathbb{E}_{\boldsymbol{\epsilon}}\left[\sum_{\ell=1}^{np} \frac{\partial \mathrm{L}_n\left(\boldsymbol{\theta}\right)}{\partial \theta_\ell} \cdot \frac{\partial(\mu_\ell + \sum_k (\mathbf{A} \otimes \mathbf{B})_{\ell,k}\epsilon_k)}{\partial B_{i,j}}\right] \\
&\overset{\text{(c)}}{=} \mathbb{E}_{\boldsymbol{\epsilon}}\left[\sum_{\ell=1}^{np} \frac{\partial \mathrm{L}_n\left(\boldsymbol{\theta}\right)}{\partial \theta_\ell} \sum_{k=1}^{np} \left(\mathbf{A} \otimes \Delta_{i,j}^{(p)}\right)_{\ell,k} \boldsymbol{\epsilon}_k\right] \\
&\overset{\text{(d)}}{=} \mathbb{E}_{\boldsymbol{\epsilon}}\left[\sum_{\ell=1}^{n}\sum_{k=1}^{n} \frac{\partial \mathrm{L}_n\left(\boldsymbol{\theta}\right)}{\partial \theta_{i+(\ell-1)n}} A_{\ell,k}\boldsymbol{\epsilon}_{j+(k-1)n}\right],
\end{aligned} \tag{57}
$$

where

- (a) is because $\boldsymbol{\theta}$ is a vector of length $n \cdot p$ and by the chain rule for derivatives;

- (b) holds since $\theta_\ell = \mu_\ell + \sum_{k=1}^{np} (\mathbf{A} \otimes \mathbf{B})_{\ell,k}\,\epsilon_k$;

- (c) is by definition of $\Delta_{i,j}^{(p)}$, and since we differentiate by $B_{i,j}$;

- (d) is since $(\mathbf{A} \otimes \Delta_{i,j}^{(p)})_{\ell,k} \neq 0$ if $k \mod n = j$ and if $\ell \mod n = i$.

13 Derivation of the fixed-point equations for the matrix variate Gaussian

In this section, we provide additional details on the derivation of the fixed-point equations for the the matrix variate Gaussian.

$$\boldsymbol{\mu} = \mathbf{m} - (\mathbf{V}_1 \otimes \mathbf{V}_2)\, \mathbb{E}_{\boldsymbol{\epsilon}}\left[\nabla \mathrm{L}_n\left(\boldsymbol{\theta}\right)\right] \tag{58}$$

$$\mathbf{A}\mathbf{A}^\top + \left(\frac{p}{\mathrm{Tr}\left(\mathbf{V}_2^{-1}\boldsymbol{\Sigma}_2\right)}\right)\mathbf{V}_1 \frac{1}{p}\mathbb{E}_{\boldsymbol{\epsilon}}\left[\boldsymbol{\Psi}^\top \mathbf{B}\boldsymbol{\Phi}\right]\mathbf{A}^\top - \left(\frac{p}{\mathrm{Tr}\left(\mathbf{V}_2^{-1}\boldsymbol{\Sigma}_2\right)}\right)\mathbf{V}_1 = 0 \tag{59}$$

$$\mathbf{B}\mathbf{B}^\top + \left(\frac{n}{\mathrm{Tr}\left(\mathbf{V}_1^{-1}\boldsymbol{\Sigma}_1\right)}\right)\mathbf{V}_2 \frac{1}{n}\mathbb{E}_{\boldsymbol{\epsilon}}\left[\boldsymbol{\Psi}\mathbf{A}\boldsymbol{\Phi}^\top\right]\mathbf{B}^\top - \left(\frac{n}{\mathrm{Tr}\left(\mathbf{V}_1^{-1}\boldsymbol{\Sigma}_1\right)}\right)\mathbf{V}_2 = 0 \tag{60}$$

Lemma 2 reveals the fixed-point equations

$$\boldsymbol{\mu} = \mathbf{m} - (\mathbf{V}_1 \otimes \mathbf{V}_2)\, \mathbb{E}_{\boldsymbol{\epsilon}}\left[\nabla \mathrm{L}_n\left(\boldsymbol{\theta}\right)\right] \tag{61}$$

$$\mathbf{A} = \mathbf{D}_1\mathbf{Q}_1 - \frac{1}{2}\left(\frac{p}{\mathrm{Tr}\left(\mathbf{V}_2^{-1}\boldsymbol{\Sigma}_2\right)}\right)\mathbf{V}_1 \frac{1}{p}\mathbb{E}_{\boldsymbol{\epsilon}}\left[\boldsymbol{\Psi}^\top \mathbf{B}\boldsymbol{\Phi}\right] \tag{62}$$

$$\mathbf{B} = \mathbf{D}_2\mathbf{Q}_2 - \frac{1}{2}\left(\frac{n}{\mathrm{Tr}\left(\mathbf{V}_1^{-1}\boldsymbol{\Sigma}_1\right)}\right)\mathbf{V}_2 \frac{1}{n}\mathbb{E}_{\boldsymbol{\epsilon}}\left[\boldsymbol{\Psi}\mathbf{A}\boldsymbol{\Phi}^\top\right] \tag{63}$$

14 Proof of Theorem 1

Proof. We define $\theta_j = \mu_j + \epsilon_j\sigma_j$ where $\epsilon_j \sim \mathcal{N}\left(0,1\right)$. According to the smoothing theorem, the following holds

$$\mathbb{E}_{\boldsymbol{\epsilon}}\left[\frac{\partial \mathrm{L}_n\left(\boldsymbol{\theta}\right)}{\partial \theta_i}\epsilon_i\right] = \mathbb{E}_{\epsilon_{j\neq i}}\left[\mathbb{E}_{\epsilon_i}\left[\frac{\partial \mathrm{L}_n\left(\boldsymbol{\theta}\right)}{\partial \theta_i}\epsilon_i \,\middle|\, \epsilon_{j\neq i}\right]\right]. \tag{64}$$

The conditional expectation is:

$$\mathbb{E}_{\epsilon_i}\left[\frac{\partial \mathrm{L}_n\left(\boldsymbol{\theta}\right)}{\partial \theta_i}\epsilon_i \,\middle|\, \epsilon_{j\neq i}\right] = \int_{-\infty}^{\infty} \frac{\partial \mathrm{L}_n\left(\boldsymbol{\theta}\right)}{\partial \theta_i}\epsilon_i f_{\epsilon_i}\left(\epsilon_i\right) d\epsilon_i, \tag{65}$$

where f_{ϵ_i} is the probability density function of a standard normal distribution. Since f_{ϵ_i} is an even function

$$\mathrm{E}_{\epsilon_i} \left[\frac{\partial \mathrm{L}_n(\boldsymbol{\theta})}{\partial \theta_i} \epsilon_i \,\middle|\, \epsilon_{j \neq i} \right] = \int\limits_0^\infty \frac{\partial \mathrm{L}_n(\mu_i + \epsilon_i \sigma_i, \theta_{-i})}{\partial \theta_i} \epsilon_i f_{\epsilon_i}(\epsilon_i) \, d\epsilon_i - \int\limits_0^\infty \frac{\partial \mathrm{L}_n(\mu_i - \epsilon_i \sigma_i, \theta_{-i})}{\partial \theta_i} \epsilon_i f_{\epsilon_i}(\epsilon_i) \, d\epsilon_i \, .$$

$$(66)$$

Now, since $\mathrm{L}_n(\boldsymbol{\theta})$ is strongly convex function with parameter $m_n > 0$ and continuously differentiable function over $\mathbb{R}^d$, the following holds $\forall \boldsymbol{\theta}_1, \boldsymbol{\theta}_2 \in \mathbb{R}^d$:

$$(\nabla \mathrm{L}_n(\boldsymbol{\theta}_1) - \nabla \mathrm{L}_n(\boldsymbol{\theta}_2))^T (\boldsymbol{\theta}_1 - \boldsymbol{\theta}_2) \geq m_n \|\boldsymbol{\theta}_1 - \boldsymbol{\theta}_2\|_2^2 \, . \tag{67}$$

For $\boldsymbol{\theta}_1, \boldsymbol{\theta}_2$ such that

$$(\boldsymbol{\theta}_1)_j = \begin{cases} (\boldsymbol{\theta}_2)_j, & j \neq i \\[2mm] \mu_i + \epsilon_i \sigma_i, & j = i \, , \end{cases} \tag{68}$$

$$(\boldsymbol{\theta}_2)_j = \begin{cases} (\boldsymbol{\theta}_1)_j, & j \neq i \\[2mm] \mu_i - \epsilon_i \sigma_i, & j = i \, , \end{cases} \tag{69}$$

the following holds:

$$\left(\frac{\partial \mathrm{L}(\boldsymbol{\theta}_1)}{\partial \theta_i} - \frac{\partial \mathrm{L}(\boldsymbol{\theta}_2)}{\partial \theta_i} \right) \epsilon_i \geq 2 m_n \sigma_i \epsilon_i^2 \, . \tag{70}$$

Therefore, substituting this inequality into (66), we obtain:

$$\mathbb{E}_\epsilon \left[\frac{\partial \mathrm{L}(\boldsymbol{\theta})}{\partial \theta_i} \epsilon_i \right] \geq m_n \sigma_i > 0 \, . \tag{71}$$

$\square$

15 FOO-VB Algorithm: Some Special Cases

In this section, we present the FOO-VB algorithms for the matrix variate Gaussian and diagonal Gaussian variants.

15.1 Matrix variate Gaussian

In the case of matrix variate Gaussian, one can write the deterministic transformation

$$\boldsymbol{\theta} = \boldsymbol{\mu} + (\mathbf{A} \otimes \mathbf{B}) \boldsymbol{\epsilon} \tag{72}$$

in matrix form

$$\mathbf{W} = \mathbf{M} + \mathbf{B} \boldsymbol{\Phi} \mathbf{A}^\top , \tag{73}$$

where $\mathbf{W}, \boldsymbol{\Phi} \in \mathbb{R}^{d_2 \times d_1}$ and $\mathrm{vec}(\mathbf{W}) = \boldsymbol{\theta}, \mathrm{vec}(\boldsymbol{\Phi}) = \boldsymbol{\epsilon}$. The deterministic transformation and the posterior update rule for the matrix variate Gaussian in the matrix form can be found in Algorithm 3.

15.2 Diagonal Gaussian

The deterministic transformation and the posterior update rule for the diagonal Gaussian can be found in Algorithm 4.

16 Implementation details

For the matrix variate version of FOO-VB, we initialize the weights by sampling from a Gaussian distribution with zero mean and a variance of $2/(n_{\mathrm{input}} + 2)$. We do so by

Algorithm 3 Methods for the matrix variate Gaussian version

$\textsc{Transform}(\boldsymbol{\epsilon}, \phi = (\mathbf{M}, \mathbf{A}, \mathbf{B}))$:

$$\mathbf{W} = \mathbf{M} + \mathbf{B}\boldsymbol{\Phi}\mathbf{A}^\top$$

$$\boldsymbol{\Sigma}_1 = \mathbf{A}\mathbf{A}^\top$$

$$\boldsymbol{\Sigma}_2 = \mathbf{B}\mathbf{B}^\top$$

$\textsc{Update}\left(\phi_{n-1} = (\mathbf{M}, \mathbf{A}, \mathbf{B}), \boldsymbol{\epsilon}^{(1..K)}, \mathbf{g}^{(1..K)}\right)$:

$$\text{vec}(\boldsymbol{\Psi}^{(k)}) = \mathbf{g}^{(k)}$$

$$\text{vec}(\boldsymbol{\Phi}^{(k)}) = \boldsymbol{\epsilon}^{(k)}$$

$$\bar{\mathbf{E}}_1 = \frac{1}{K}\sum_{k=1}^{K} \boldsymbol{\Psi}^{(k)}$$

$$\bar{\mathbf{E}}_2 = \frac{1}{K}\sum_{k=1}^{K} \frac{1}{p}\boldsymbol{\Psi}^{(k)\top}\mathbf{B}\boldsymbol{\Phi}^{(k)}$$

$$\bar{\mathbf{E}}_3 = \frac{1}{K}\sum_{k=1}^{K} \frac{1}{n}\boldsymbol{\Psi}^{(k)\top}\mathbf{A}\boldsymbol{\Phi}^{(k)}$$

$$\mathbf{M} \leftarrow \mathbf{M} - \mathbf{B}\mathbf{B}^\top\bar{\mathbf{E}}_1\mathbf{A}\mathbf{A}^\top$$

$\mathbf{A} \leftarrow \mathbf{X}$ such that $\mathbf{X}\mathbf{X}^\top + \mathbf{A}\mathbf{A}^\top\bar{\mathbf{E}}_2\mathbf{X}^\top - \mathbf{A}\mathbf{A}^\top = 0$

$\mathbf{B} \leftarrow \mathbf{X}$ such that $\mathbf{X}\mathbf{X}^\top + \mathbf{B}\mathbf{B}^\top\bar{\mathbf{E}}_3\mathbf{X}^\top - \mathbf{B}\mathbf{B}^\top = 0$

(The matrix equations are solved using Lemma 2)

Algorithm 4 Methods for the diagonal Gaussian version

TRANSFORM$(\epsilon, \phi = (\boldsymbol{\mu}, \boldsymbol{\sigma}))$:

$$\theta_i = \mu_i + \sigma_i \epsilon_i$$

UPDATE$\left(\phi_{n-1} = (\boldsymbol{\mu}, \boldsymbol{\sigma}), \boldsymbol{\epsilon}^{(1..K)}, \mathbf{g}^{(1..K)}\right)$**:**

$$\left(\bar{\mathbf{E}}_1\right)_i = \tfrac{1}{K} \sum_{k=1}^{K} \mathbf{g}_i^{(k)}$$

$$\left(\bar{\mathbf{E}}_2\right)_i = \tfrac{1}{K} \sum_{k=1}^{K} \mathbf{g}_i^{(k)} \boldsymbol{\epsilon}_i^{(k)}$$

$$\mu_i \leftarrow \mu_i - \sigma_i^2 (\bar{\mathbf{E}}_1)_i$$

$$\sigma_i \leftarrow \sigma_i \sqrt{1 + \left(\tfrac{1}{2} \sigma_i (\bar{\mathbf{E}}_2)_i\right)^2} - \tfrac{1}{2} \sigma_i^2 (\bar{\mathbf{E}}_2)_i$$

---

sampling the mean of the wights from a Gaussian distribution, such that

$$\mathbf{M}_{i,j} \sim \mathcal{N}\left(0, \frac{2\alpha}{n_{\text{input}} + 2}\right), \tag{74}$$

where $\alpha \in (0, 1)$. In addition, we sample the diagonal elements of the matrices $\mathbf{A}, \mathbf{B}$ form a Gaussian distribution, such that

$$\epsilon_i \mathbf{A}_{i,i} \sim \mathcal{N}\left(0, \sqrt{\frac{2(1-\alpha)}{n_{\text{input}} + 2}}\right) \tag{75}$$

$$\epsilon_i \mathbf{B}_{i,i} \sim \mathcal{N}\left(0, \sqrt{\frac{2(1-\alpha)}{n_{\text{input}} + 2}}\right), \tag{76}$$

where the non-diagonal elements are initialized to zero. We use 2500 Monte Carlo samples to estimate the expected gradient during training, and average the accuracy of 2500 sampled networks during testing, unless stated otherwise.

For the diagonal version of FOO-VB, we initialize the mean of the weights μ by sampling from a Gaussian distribution with a zero mean and a variance of $2/(n_{\text{input}} +$

n_{output}), unless stated otherwise. We use 10 Monte Carlo samples to estimate the expected gradient during training, and set the weights to the learned mean testing.

16.1 Discrete permuted MNIST

We use a fully connected neural network with 2 hidden layers of 100 width, ReLUs as activation functions and softmax output layer with 10 units. We used mini-batch of size 128 and 20 epochs We conducted a hyper-parameter search for all algorithms and present the best test accuracy for 10 tasks, with $LR \in \{0.1, 0.01, 0.001, 0.0001\}$ and regularization coefficient $\in \{250, 150, 10, 0.1, 0.02\}$ (see tables 2, 3 and 4). For FOO-VB we used $\alpha = 0.5$ in the matrix variate version, and $\sigma_{init} = 0.047$ in the diagonal version. For Online EWC we used LR of 0.001 and regularization coefficient of 10.0 and for MAS we used LR of 0.001 and regularization coefficient of 0.1.

16.2 Continuous permuted MNIST

We use a fully connected network with 2 hidden layers of width 200. Following Hsu et al. (2018), the original MNIST images are padded with zeros to match size of 32×32. The batch size is 128, and we sample with replacement due to the properties of the continuous scenario (no definition for epoch as task boundaries are undefined). We conducted a hyper-parameter search for all algorithms and present the best test accuracy for 10 tasks, see Figure 6. For FOO-VB we used $\alpha = 0.6$ in the matrix variate version, and $\sigma_{init} = 0.06$ in the diagonal version. For Online EWC and MAS we used the following combinations of hyper-parameters: LR of 0.01 and 0.0001, regularization coefficient of 10, 0.1, 0.001, 0.0001, and optimizer SGD and Adam. The best results for

online EWC were achieved using LR of 0.01, regularization coefficient of 0.1 and SGD

optimizer. For MAS, best results achieved using LR of 0.01, regularization coefficient of
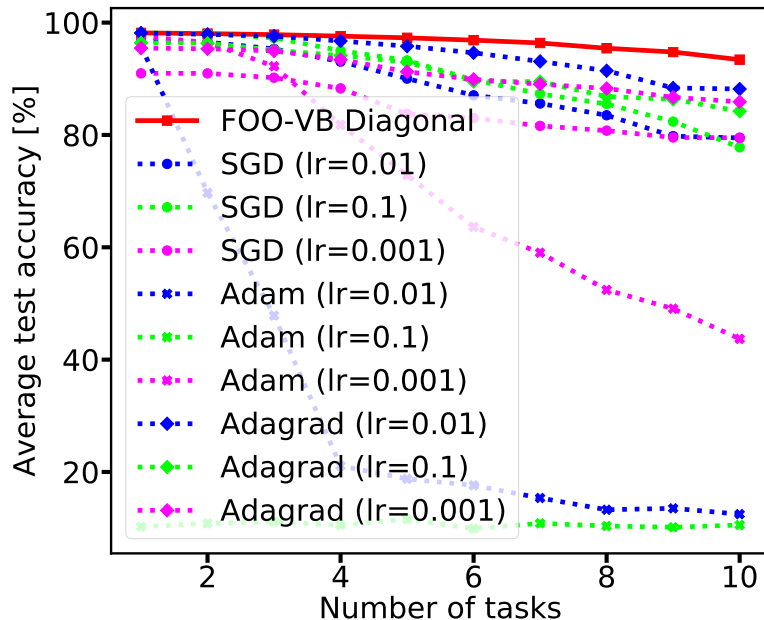
0.001 and SGD optimizer.

Figure 6: Hyper-parameters search for continuous permuted MNIST experiment.

16.3 Vision datasets mix

We followed the experiment as described in Ritter et al. (2018). We use a batch size of

64, and we normalize the datasets to have zero mean and unit variance. The network

architecture is LeNet like with 2 convolution layers with 20 and 50 channels and kernel

size of 5, each convolution layer is followed by a Relu activations function and max pool,

and the two layers are followed with fully connected layer of size 500 before the last

layer. SGD baseline was trained with a constant learning rate of 0.001 and ADAM used

$\epsilon = 10^{-8}$, LR of 0.001 and $(\beta_1, \beta_2) = (0.9, 0.999)$. FOO-VD trained with initial STD

of 0.02 and batch size 64.

17 Complexity

The diagonal version of FOO-VB requires $\times 2$ more parameters compared to SGD, as it stores both the mean and the STD per weight. In terms of time complexity, the major difference between SGD and FOO-VB arises from the estimation of the expected gradients using Monte Carlo samples during training. Since those Monte Carlo samples are completely independent the algorithm is embarrassingly parallel.

Specifically, given a mini-batch: for each Monte Carlo sample, FOO-VB generates a random network using μ and σ, then making a forward-backward pass with the randomized weights.

Two main implementation methods are available (using 10 Monte Carlo samples as an example):

1. Producing the (10) Monte Carlo samples sequentially, thus saving only a single randomized network in memory at a time (decreasing memory usage, increasing runtime).

2. Producing the (10) Monte Carlo samples in parallel, thus saving (10) randomized networks in memory (increasing memory usage, decreasing runtime).

We analyzed how the number of Monte Carlo iterations affects the runtime on Continuous permuted MNIST using the first method of implementation (sequential MC samples). The results, reported in Table 1, show that runtime is indeed a linear function of the number of MC iterations.

43

Table 1: Average runtime of a single training epoch with different numbers of Monte Carlo samples. The MC iterations have linear effect on runtime for classification, and almost no effect in the continuous task-agnostic experiment, probably due to implementation specifics. Using less MC iterations does not affect accuracy significantly. Accuracy reported in the table is from the continuous experiment (Fig 5).

Experiment	MC iterations	Accuracy	Iteration runtime [seconds]	Vs. SGD
Continuous	SGD	77.79 %	0.0024	×1
task-agnostic	2 (FOO-VB)	92 %	0.0075	× 3.12
(Fig 5)	10 (FOO-VB)	93.40%	0.0287	× 11.95

For the matrix variate version of FOO-VB, the main bottleneck is the SVD operation, with the following breakdown:

- A single MC iteration takes 0.002 seconds

- A single iteration (including all MC iterations and the matrix updates) takes 0.68 seconds (with 10 MC iterations)

- Each SVD takes 0.22 seconds, in this case we have two SVDs, which takes 0.44 seconds - about $\frac{2}{3}$ of the iteration runtime.

In the experiments we used a single GPU (GeForce GTX 1080 Ti).

Table 2: Hyper-parameter search results on discrete permuted MNIST - EWCOnline

Algorithm	LR	Regularization coef.	Accuracy
EWConline	0.01	250.0	38.47
EWConline	0.01	150.0	48.33
EWConline	0.01	10.0	81.33
EWConline	0.01	0.1	42.46
EWConline	0.01	0.02	39.40
EWConline	0.0001	250.0	46.70
EWConline	0.0001	150.0	55.58
EWConline	0.0001	10.0	84.03
EWConline	0.0001	0.1	58.68
EWConline	0.0001	0.02	55.17
EWConline	0.001	250.0	46.20
EWConline	0.001	150.0	54.19
EWConline	0.001	10.0	85.06
EWConline	0.001	0.1	52.13
EWConline	0.001	0.02	40.48
EWConline	0.1	250.0	19.32
EWConline	0.1	150.0	29.05
EWConline	0.1	10.0	10.04
EWConline	0.1	0.1	10.49
EWConline	0.1	0.02	9.688

Table 3: Hyper-parameter search results on discrete permuted MNIST - MAS

Algorithm	LR	Regularization coef.	Accuracy
MAS	0.01	250.0	29.73
MAS	0.01	150.0	29.85
MAS	0.01	10.0	44.20
MAS	0.01	0.1	63.50
MAS	0.01	0.02	63.46
MAS	0.0001	250.0	49.57
MAS	0.0001	150.0	54.13
MAS	0.0001	10.0	78.03
MAS	0.0001	0.1	83.49
MAS	0.0001	0.02	75.32
MAS	0.001	250.0	46.41
MAS	0.001	150.0	50.64
MAS	0.001	10.0	72.59
MAS	0.001	0.1	84.56
MAS	0.001	0.02	82.63
MAS	0.1	250.0	8.948
MAS	0.1	150.0	9.772
MAS	0.1	10.0	13.64
MAS	0.1	0.1	21.45
MAS	0.1	0.02	19.49

Table 4: Hyper-parameter search results on discrete permuted MNIST - Adam, SGD and Adagrad

Algorithm	LR	Regularization coef.	Accuracy
Adam	0.0001	0.0	52.64
Adam	0.01	0.0	10.69
Adam	0.1	0.0	10.31
Adam	0.001	0.0	27.20
SGD	0.01	0.0	66.18
SGD	0.0001	0.0	71.17
SGD	0.001	0.0	76.94
SGD	0.1	0.0	36.97
Adagrad	0.1	0.0	51.48
Adagrad	0.001	0.0	82.42
Adagrad	0.0001	0.0	74.14
Adagrad	0.01	0.0	75.98

18 5000 epochs training

We turn to a MNIST classification experiment to demonstrate the convergence of the log-likelihood cost function and the histogram of STD values. We train a fully connected neural network with two hidden layers and layer width of 400 for 5000 epochs.
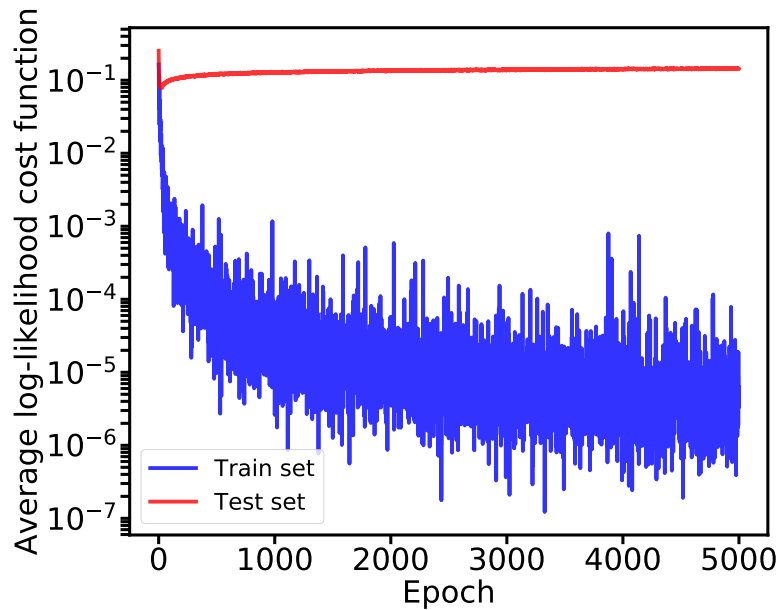

Figure 7: Average log-likelihood cost function of the train set and the test set - layer width 400.

Figure 7 shows the log-likelihood cost function of the training set and the test set. As can be seen, the log-likelihood cost function on the training set decreases during the training process and converges to a low value. Thus, FOO-VB does not experience underfitting and over-pruning as was shown by Trippe and Turner (2018) for BBB (Blundell et al., 2015).

Figure 8 shows the histogram of STD values during the training process. As can be seen, the histogram of STD values converges. This demonstrates that σ_i does not
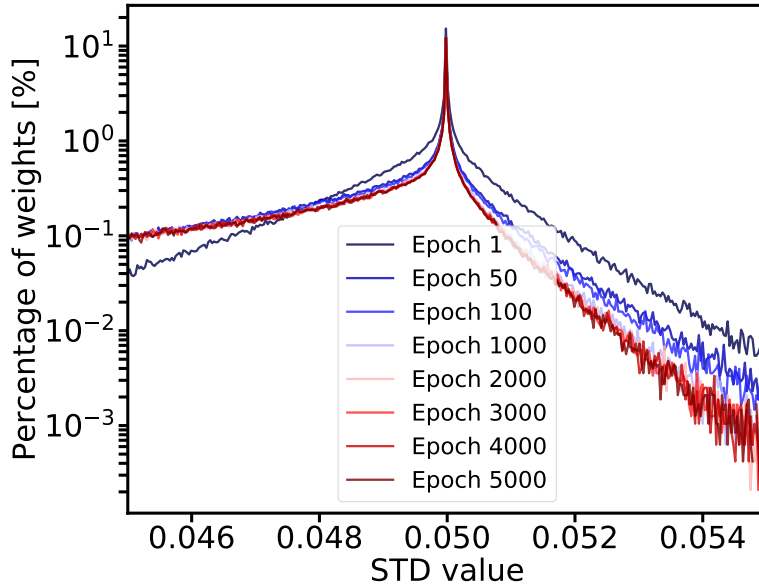
Figure 8: Histogram of STD values, the initial STD value is 0.05.

collapse to zero even after 5000 epochs.

Figure 9 shows the learning curve of the train set and the test set. As can be seen, the test accuracy does not drop even if we continue to train for 5000 epochs.

19 Task-aware continual learning on vision datasets

We followed Ritter et al. (2018) and challenged our algorithm with the vision datasets experiment. In this experiment, we train sequentially on MNIST, notMNIST, [4] Fashion-MNIST, SVHN and CIFAR10 (LeCun et al., 1998; Xiao et al., 2017; Netzer et al., 2011;

[4]Originally published at

http://yaroslavvb.blogspot.co.uk/2011/09/notmnist-dataset.html and downloaded from

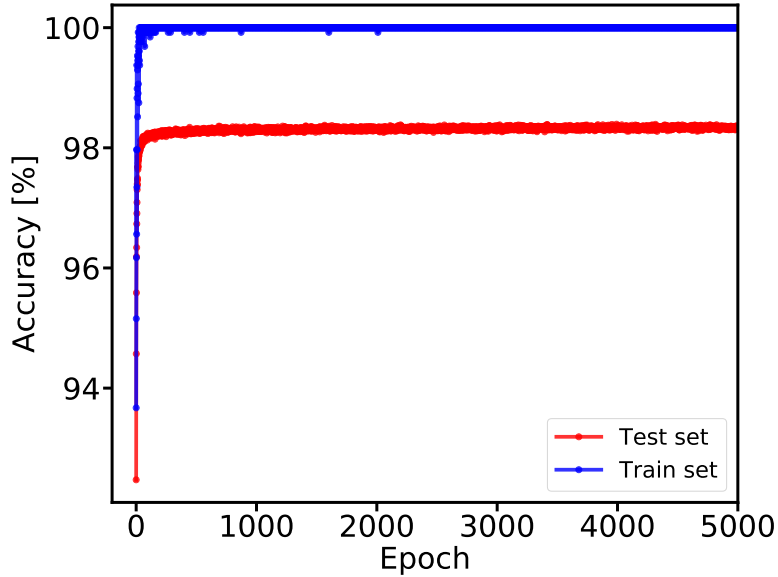https://github.com/davidflanagan/notMNIST-to-MNIST

Figure 9: Test accuracy and train accuracy - layer width 400.

Krizhevsky and Hinton, 2009). Training is done in a sequential way with 20 epochs per task — in epochs 1-20 we train on MNIST (first task), and on epochs 81-100 we train on CIFAR10 (last task). All five datasets consist of about 50,000 training images from 10 different classes, but they differ from each other in various ways: black and white vs. RGB, letters and digits vs. vehicles and animals etc. We use the exact same setup as in Ritter et al. (2018) for the comparison — LeNet-like (LeCun et al., 1998) architecture with separated last layer for each task as in CIFAR10/CIFAR100 experiment. Results are reported on Table 5.

Table 5: Accuracy for each task after training sequentially on all tasks. PTL stands for Per-Task Laplace (one penalty per task), AL is Approximate Laplace (Laplace approximation of the full posterior at the mode of the approximate objective) and OL is Online Laplace approximation. Results for SI, PTL, AL and OL are as reported in Ritter et al. (2018). We highlight the best accuracy in bold.

Test accuracy [%] on the end of last task (CIFAR10)

Method	Average	MNIST	notMNIST	F-MNIST	SVHN	CIFAR10
Diagonal methods						
FOO-VB	81.37	86.42	89.23	83.05	**82.21**	**65.96**
SGD	69.64	84.79	82.12	65.91	52.31	63.08
ADAM	29.67	17.39	26.26	25.02	15.10	64.62
SI	77.21	87.27	79.12	84.61	77.44	57.61
PTL	**82.96**	**97.83**	**94.73**	89.13	79.80	53.29
AL	82.55	96.56	92.33	**89.27**	78.00	56.57
OL	82.71	96.48	93.41	88.09	81.79	53.80
Non-Diagonal methods						
PTL	85.32	97.85	**94.92**	89.31	**85.75**	58.78
AL	85.35	**97.90**	94.88	90.08	85.24	58.63
OL	**85.40**	97.17	94.78	**90.36**	85.59	**59.11**

References

Achille, A., Eccles, T., Matthey, L., Burgess, C., Watters, N., Lerchner, A., and Higgins, I. (2018). Life-long disentangled representation learning with cross-domain latent homologies. In *Advances in Neural Information Processing Systems*, pages 9873–9883.

Aljundi, R., Babiloni, F., Elhoseiny, M., Rohrbach, M., and Tuytelaars, T. (2018). Memory aware synapses: Learning what (not) to forget. In *European Conference on Computer Vision*, pages 144–161. Springer.

Aljundi, R., Lin, M., Goujaud, B., and Bengio, Y. (2019). Gradient based sample selection for online continual learning. In *Advances in Neural Information Processing Systems*, pages 11816–11825.

Amari, S.-I. (1998). Natural gradient works efficiently in learning. *Neural computation*, 10(2):251–276.

Balan, A. K., Rathod, V., Murphy, K. P., and Welling, M. (2015). Bayesian dark knowledge. In *Advances in Neural Information Processing Systems*, pages 3438–3446.

Berry, M. and Sameh, A. (1989). An overview of parallel algorithms for the singular value and symmetric eigenvalue problems. *Journal of Computational and Applied Mathematics*, 27(1):191 – 213. Special Issue on Parallel Algorithms for Numerical Linear Algebra.

Bishop, C. M. et al. (1995). *Neural networks for pattern recognition*. Oxford university press.

Blundell, C., Cornebise, J., Kavukcuoglu, K., and Wierstra, D. (2015). Weight uncertainty in neural networks. *arXiv preprint arXiv:1505.05424*.

Broderick, T., Boyd, N., Wibisono, A., Wilson, A. C., and Jordan, M. I. (2013). Streaming variational bayes. In *Advances in Neural Information Processing Systems*, pages 1727–1735.

Chaudhry, A., Dokania, P. K., Ajanthan, T., and Torr, P. H. (2018). Riemannian walk for incremental learning: Understanding forgetting and intransigence. *arXiv preprint arXiv:1801.10112*.

Cseke, B., Opper, M., and Sanguinetti, G. (2013). Approximate inference in latent gaussian-markov models from continuous time observations. In Burges, C. J. C., Bottou, L., Welling, M., Ghahramani, Z., and Weinberger, K. Q., editors, *Advances in Neural Information Processing Systems*, volume 26, pages 971–979. Curran Associates, Inc.

Dauphin, Y., Pascanu, R., Gulcehre, C., Cho, K., Ganguli, S., and Bengio, Y. (2014). Identifying and attacking the saddle point problem in high-dimensional non-convex optimization. *NIPS*, pages 1–9.

Finn, C., Abbeel, P., and Levine, S. (2017). Model-agnostic meta-learning for fast adaptation of deep networks. In Precup, D. and Teh, Y. W., editors, *Proceedings of the 34th International Conference on Machine Learning*, volume 70 of *Proceedings*

of Machine Learning Research, pages 1126–1135, International Convention Centre, Sydney, Australia. PMLR.

Gelman, A., Carlin, J. B., Stern, H. S., Dunson, D. B., Vehtari, A., and Rubin, D. B. (2013). *Bayesian data analysis*. Chapman and Hall/CRC.

Graves, A. (2011). Practical variational inference for neural networks. In *Advances in neural information processing systems*, pages 2348–2356.

Gupta, A. K. and Nagar, D. K. (2018). *Matrix variate distributions*. Chapman and Hall/CRC.

He, X., Sygnowski, J., Galashov, A., Rusu, A. A., Teh, Y. W., and Pascanu, R. (2019). Task agnostic continual learning via meta learning.

Hernández-Lobato, J. M. and Adams, R. (2015). Probabilistic backpropagation for scalable learning of bayesian neural networks. In *International Conference on Machine Learning*, pages 1861–1869.

Hernández-Lobato, J. M., Li, Y., Rowland, M., Hernández-Lobato, D., Bui, T., and Turner, R. E. (2016). Black-box α-divergence minimization.

Hinton, G. E. and Camp, D. V. (1993). Keeping the neural networks simple by minimizing the description length of the weights. In *COLT '93*.

Hsu, Y.-C., Liu, Y.-C., and Kira, Z. (2018). Re-evaluating continual learning scenarios: A categorization and case for strong baselines. *arXiv preprint arXiv:1810.12488*.

Khan, M. E., Nielsen, D., Tangkaratt, V., Lin, W., Gal, Y., and Srivastava, A. (2018). Fast

and scalable bayesian deep learning by weight-perturbation in adam. *arXiv preprint arXiv:1806.04854*.

Kingma, D. P. and Welling, M. (2013). Auto-encoding variational bayes. *arXiv preprint arXiv:1312.6114*.

Kirkpatrick, J., Pascanu, R., Rabinowitz, N., Veness, J., Desjardins, G., Rusu, A. A., Milan, K., Quan, J., Ramalho, T., Grabska-Barwinska, A., et al. (2017). Overcoming catastrophic forgetting in neural networks. *Proceedings of the National Academy of Sciences*, 114(13):3521–3526.

Knowles, D. and Minka, T. (2011). Non-conjugate variational message passing for multinomial and binary regression. In Shawe-Taylor, J., Zemel, R., Bartlett, P., Pereira, F., and Weinberger, K. Q., editors, *Advances in Neural Information Processing Systems*, volume 24, pages 1701–1709. Curran Associates, Inc.

Krizhevsky, A. and Hinton, G. (2009). Learning multiple layers of features from tiny images.

Kurle, R., Cseke, B., Klushyn, A., van der Smagt, P., and Günnemann, S. (2019). Continual learning with bayesian neural networks for non-stationary data. In *International Conference on Learning Representations*.

LeCun, Y., Bottou, L., Bengio, Y., and Haffner, P. (1998). Gradient-based learning applied to document recognition. *Proceedings of the IEEE*, 86(11):2278–2324.

Lee, S., Kim, J., Ha, J., and Zhang, B. (2017). Overcoming catastrophic forgetting by incremental moment matching.

Li, Z. and Hoiem, D. (2017). Learning without forgetting. *IEEE Transactions on Pattern Analysis and Machine Intelligence*.

MacKay, D. J. C. (1992). A practical Bayesian framework for backpropagation networks. *Neural computation*, 472(1):448–472.

Martens, J. and Grosse, R. (2015). Optimizing neural networks with kronecker-factored approximate curvature. In *International conference on machine learning*, pages 2408–2417.

McCloskey, M. and Cohen, N. J. (1989). Catastrophic interference in connectionist networks: The sequential learning problem. In *Psychology of learning and motivation*, volume 24, pages 109–165. Elsevier.

Nagabandi, A., Finn, C., and Levine, S. (2018). Deep online learning via meta-learning: Continual adaptation for model-based rl. *arXiv preprint arXiv:1812.07671*.

Neal, R. M. (1994). *Bayesian Learning for Neural Networks*. PhD thesis, Dept. of Computer Science, University of Toronto.

Netzer, Y., Wang, T., Coates, A., Bissacco, A., Wu, B., and Ng, A. Y. (2011). Reading digits in natural images with unsupervised feature learning. In *NIPS workshop on deep learning and unsupervised feature learning*, volume 2011, page 5.

Nguyen, C. V., Li, Y., Bui, T. D., and Turner, R. E. (2017). Variational continual learning. *arXiv preprint arXiv:1710.10628*.

Opper, M. and Archambeau, C. (2009). The variational gaussian approximation revisited. *Neural computation*, 21(3):786–792.

Parisi, G. I., Kemker, R., Part, J. L., Kanan, C., and Wermter, S. (2018). Continual lifelong learning with neural networks: A review. *arXiv preprint arXiv:1802.07569.*

Poloni, F. (2018). Non linear matrix equation. MathOverflow.

Rao, D., Visin, F., Rusu, A., Pascanu, R., Teh, Y. W., and Hadsell, R. (2019). Continual unsupervised representation learning. In *Advances in Neural Information Processing Systems*, pages 7645–7655.

Ritter, H., Botev, A., and Barber, D. (2018). Online structured laplace approximations for overcoming catastrophic forgetting. *arXiv preprint arXiv:1805.07810.*

Rusu, A. A., Rabinowitz, N. C., Desjardins, G., Soyer, H., Kirkpatrick, J., Kavukcuoglu, K., Pascanu, R., and Hadsell, R. (2016). Progressive neural networks. *arXiv preprint arXiv:1606.04671.*

Schwarz, J., Luketina, J., Czarnecki, W. M., Grabska-Barwinska, A., Teh, Y. W., Pascanu, R., and Hadsell, R. (2018). Progress & compress: A scalable framework for continual learning. *arXiv preprint arXiv:1805.06370.*

Sheth, R. and Khardon, R. (2016). A fixed-point operator for inference in variational bayesian latent gaussian models. In Gretton, A. and Robert, C. C., editors, *Proceedings of the 19th International Conference on Artificial Intelligence and Statistics*, volume 51 of *Proceedings of Machine Learning Research*, pages 761–769, Cadiz, Spain. PMLR.

Shin, H., Lee, J. K., Kim, J., and Kim, J. (2017). Continual learning with deep generative replay. In *Advances in Neural Information Processing Systems*, pages 2990–2999.

Soudry, D., Hubara, I., and Meir, R. (2014). Expectation backpropagation: Parameter-free training of multilayer neural networks with continuous or discrete weights. In *Advances in Neural Information Processing Systems*, pages 963–971.

Thanh-Tung, H. and Tran, T. (2018). On catastrophic forgetting and mode collapse in generative adversarial networks.

Trippe, B. and Turner, R. (2018). Overpruning in variational bayesian neural networks. *arXiv preprint arXiv:1801.06230*.

Welling, M. and Teh, Y. W. (2011). Bayesian learning via stochastic gradient langevin dynamics. In *Proceedings of the 28th International Conference on Machine Learning (ICML-11)*, pages 681–688.

Xiao, H., Rasul, K., and Vollgraf, R. (2017). Fashion-mnist: a novel image dataset for benchmarking machine learning algorithms. *arXiv preprint arXiv:1708.07747*.

Zenke, F., Poole, B., and Ganguli, S. (2017). Continual learning through synaptic intelligence. In *International Conference on Machine Learning*, pages 3987–3995.

Zeno, C., Golan, I., Hoffer, E., and Soudry, D. (2019). Task agnostic continual learning using online variational bayes.

Zhang, G., Sun, S., Duvenaud, D., and Grosse, R. (2017). Noisy natural gradient as variational inference. *arXiv preprint arXiv:1712.02390*.